AN ABSTRACT OF THE THESIS OF

Margo Kaller for the degree of Master of Science in Microbiology presented on May 22nd, 2014.

Title: Evaluation of Peptide Phosphorodiamidate Morpholino Oligomers as a Novel Antibiotic Therapy.

Abstract approved:

_____

Bruce L. Geller

Peptide-phosphorodiamidate morpholino oligomers (PPMOs) are synthetic DNA mimics that bind and silence gene targets. Through designing PPMOs that silence essential or resistance genes in pathogens, these antisense oligomers could be utilized as novel antimicrobials. Towards this end, my thesis employed minimum inhibitory concentration assays (MICs) to identify PPMOs capable of inhibiting *in vitro* growth of *E. coli*. Quantitative real-time PCR was then used to elucidate PPMO mechanism through investigating transcriptional effects of PPMO treatment. Lastly, tissue culture cytotoxicity tests were performed to ensure PPMO were benign for human cells. My thesis has identified multiple PPMOs capable of silencing the essential gene *acpP* and the resistance gene *NDM-1*, establishing a foundation for both independent and combination PPMO antibiotic treatments. My work has also shown PPMO treatment to not significantly affect transcription of target genes, suggesting PPMOs to exert their effects entirely through translational regulation. Finally, the tissue culture assays demonstrates PPMOs to be nontoxic to human cells. Taken together, these data indicate PPMOs are a safe, adaptable, and effective new option for antibiotic therapy.

Evaluation of Peptide Phosphorodiamidate Morpholino Oligomers As A Novel Antibiotic Therapy

by
Margo Kaller

A THESIS

submitted to

Oregon State University

in partial fulfillment of
the requirements for the
degree of

Master of Science

Presented May 22nd, 2014
Commencement June 2014

Master of Science thesis of Margo Kaller presented on May 22nd, 2014

APPROVED:

Major Professor, representing Microbiology

Chair of the Department of Microbiology

Dean of the Graduate School

I understand that my thesis will become part of the permanent collection of Oregon State University libraries. My signature below authorizes release of my thesis to any reader upon request.

Margo Kaller, Author

ACKNOWLEDGEMENTS

I am grateful above all to my mother, Susan Kaller. Without her endless support and loving guidance, I would have felt truly adrift and uncertain as I tried to make my way through graduate school.

I also want to express my deepest affection for my close friends Roberto Garcia III, Stephanie Rosales, and Wei Wei. Sharing so much laughter, commiseration, and tasty food with these kind and excellent people made every day something to look forward to throughout the ups and downs of my thesis work. Knowing them has changed my perspective on human relationships quite a bit, and I am grateful for the insights I have received.

I am very thankful to my mentor Dr. Bruce Geller for his teaching, advice, and inspiration in this project. Dr. Janine Trempy has been a tremendous motivator for me to get my writing done, and so I am appreciative of her guidance as well! Dr. Siva Kolluri's class on molecular therapeutics was a formative experience for my analytical skills, and so I am deeply thankful for his teaching and support of my future endeavors. Finally, I want to thank Dr. Alan Bakalinsky for taking the time to evaluate this work as part of my thesis committee. I am grateful for the hard work and patience of my thesis committee as they help me through this last refinement of my research mentality.

TABLE OF CONTENTS

LIST OF FIGURES

CHAPTER 1 - INTRODUCTION

Increasing resistance to antibiotic therapies is a common problem across diverse populations of bacterial pathogens. Single and multi-drug resistance has been exhibited by such wide-ranging organisms as *Staphylococcus aureus, Enterococcus faecium, Streptococcus pneumoniae, Klebsiella pneumoniae, Salmonella typhimurium,* and *Mycobacterium tuberculosis,* as well as *Acinetobacter* and *Escherichia* species. In addition, these pathogens have also given rise to extremely resistant strains lacking sensitivity to all known antimicrobial compounds. The ubiquitous emergence of antibiotic resistance has become a source of significant morbidity/mortality both for immunocompromised individuals in the hospital setting and healthy individuals outside clinical environments (Boucher et al., 2013; Tenover, 2001). The widespread loss of health or life incurred by antimicrobial resistance also places a large economic burden on the United States. Current studies estimate infections by resistant infections to cost $20 billion per year in health service expenses and $30 billion per year for lost productivity (Smith and Coast, 2013). To combat the spread of antimicrobial resistance, multiple clinical practices and educational campaigns have made efforts towards reducing the trend for antibiotic over-prescription (Costelloe et al., 2010). Although the excessive use of antibiotics is an important source of natural selection for resistant pathogens, reducing treatment is only a partial solution to the larger problem of decreasingly effective antimicrobial drugs (Giedraitiene et al., 2011). To address the issue of widespread drug resistance, potent new antimicrobial agents must be developed.

However, the high cost of drug discovery and low profitability of antimicrobial therapies has severely stagnated research into novel antibiotic

compounds. Only two new antibiotics have been approved for marketing in the United States in the last four years, and the number of potential antibiotics being evaluated in the clinical pipeline continues to decrease (Boucher et al., 2013; Fischbach and Walsh, 2009). None of the new antibiotics approved in the last 20 years is approved for parenteral use against Gram-negative bacteria. Additionally, most 'novel' antibiotic drugs developed since the 1960s are only slight modifications of chemical scaffolds that were first introduced more than half a century ago (Figure 1). Modifications for only four of these scaffolds – penicillins, cephalosporins, quinolones, and macrolides – constitute three-quarters of all patents filed for new antibiotics in the last thirty years (Fischbach and Walsh, 2009). This method of

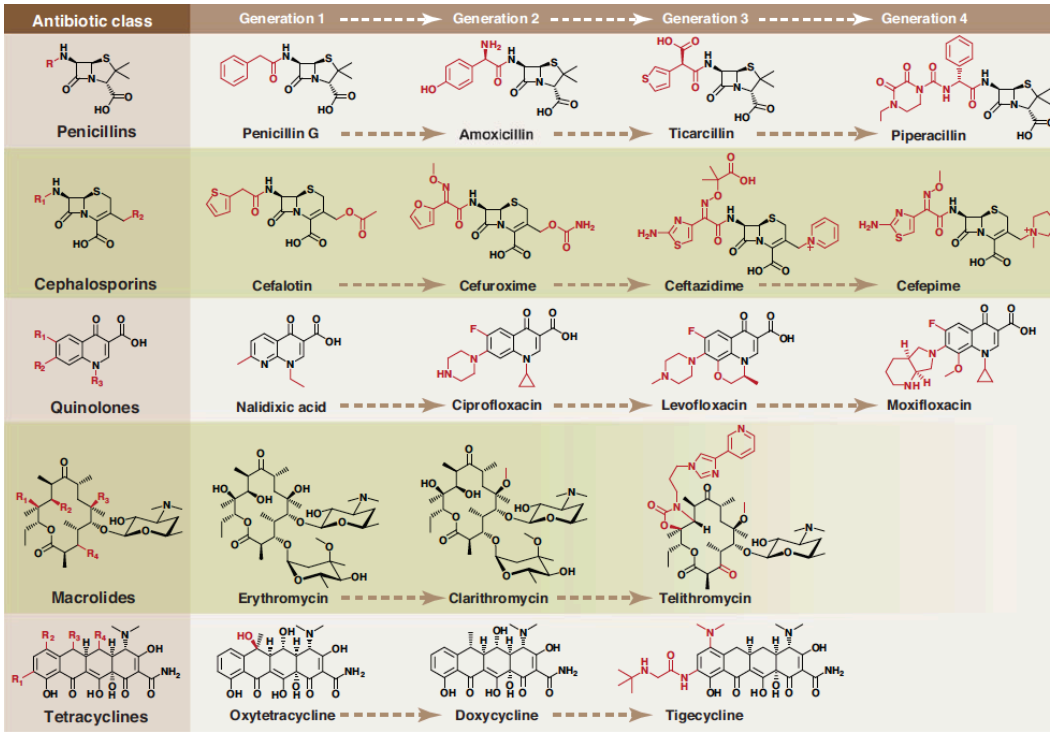

Figure 1. **Standard Antibiotic Scaffolds** Generations of antibiotic development are predicated upon minor changes to essentially similar structures. Scaffolds are outline in black, modifications are outlined in red (Fischbach and Walsh, 2009).

antibiotic design enables pathogens to quickly develop resistances to any ‘new’ drugs the same way they became resistant to the previous generation of standard antibiotics. Bacteria that previously resisted one generation need only alter themselves slightly to resist the next. Bacterial familiarity with current antibiotic structures and targets necessitates new compounds with foreign structures and markedly different ligands.

Clearly a new strategy of antibiotic discovery is urgently needed. One such strategy is a technology that uses synthetic nucleic acid-like oligomers to silence expression of bacterial genes. The sequence of bases in these oligomers can be programmed during synthesis, so that a virtually unlimited number of novel oligomers can be screened easily and rapidly.

CHAPTER 2 – LITERATURE REVIEW

Peptide-conjugated phosphorodiamidate morpholino oligomers (PPMO) are one kind of antisense oligonucleotides, a type of synthetic compound designed to mimic the structure of DNA. PPMOs have the same four bases as DNA but the linkage between bases is modified (Figure 2). The deoxyribose ring is replaced with a morpholino ring, and the phosphodiester bonds are substituted with phosphorodiamidate bonds. The modified linkage allows the bases to hydrogen bond with single-stranded RNA by complementary base-pairing, but prevents degradation by nucleases. A membrane-penetrating peptide is attached to either of the ends, which is required for transit through the outer membrane of Gram-negative bacteria.

PPMOs bind to specific mRNAs and interfere with translation. PPMOs targeted to essential genes prevent growth and are bactericidal (Greenberg et al., 2010; Geller et al., 2005; Geller et al., 2013; Mellbye et al., 2009; Tilley et al., 2007; Umland

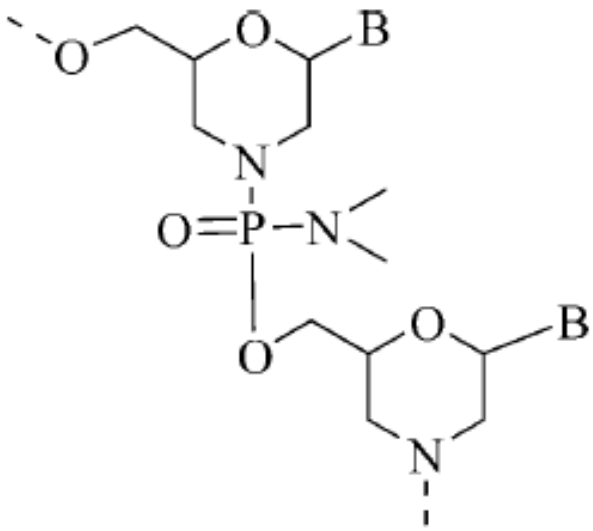

Figure 2. **PPMO Scaffold** The general structure for phosphorodiamidate morpholino oligomers' active site. PMOs are conjugated to amphipathic polypeptides, which enable them to penetrate of the bacterial cell wall (Geller et al., 2003). The "B" represents any of the four bases found in DNA.

et al., 2012). PPMOs' ability to target bacterial genes constitutes these compounds' most significant advantage relative to classical antibiotics. Many currently available antimicrobials rely on post-translational targets like polymerases and peptidases, which can be readily modified with minimal cost to the pathogen itself (Tillotson and Theriault, 2013). By contrast, the bacterial gene targets of PPMOs could be very difficult for the pathogen to mutate without incurring deleterious effects. PPMOs' design as DNA mimics also provides flexibility to target any gene of interest by simply changing a few of the compound's synthetic nucleobases. Targets for current antibiotic therapies are significantly more constrained since the classical compounds' scaffolds are necessarily conserved for efficacy (Fischbach and Walsh, 2009). Finally, the gene targets of PPMOs enable an extremely specific approach to antimicrobial therapy. Current antibiotics are plagued by the risk of adverse secondary reactions when drugs bind a target ligand present in both the pathogen and the commensal flora. Since PPMOs can target genes unique to the invading microbe, these antisense oligomers are less likely to induce the side effects of broad-spectrum antibiotics. Taken together, PPMOs' readily customizable sequences and precise, potent mechanisms of action render these compounds promising candidates for novel antibiotic therapies.

Design and Mechanism of Antisense Oligomers

PPMOs are the most recently developed class of antisense oligonucleotides, a diverse family of compounds evaluated over the past few decades for their gene-silencing ability. As artificial mimics of DNA molecules, compounds in the antisense oligonucleotide family are characterized by their ability to base-pair with unique

nucleotide sequences on mRNA transcripts from the gene of interest. Once the antisense oligonucleotide has bound its target mRNA sequence, the double-stranded RNA created by the synthetic compound's hybridization either prevents formation of the 70S ribosome or interferes with translocation, thereby blocking translation (Figure 3). The translational arrest resultant from antisense oligomer hybridization stably

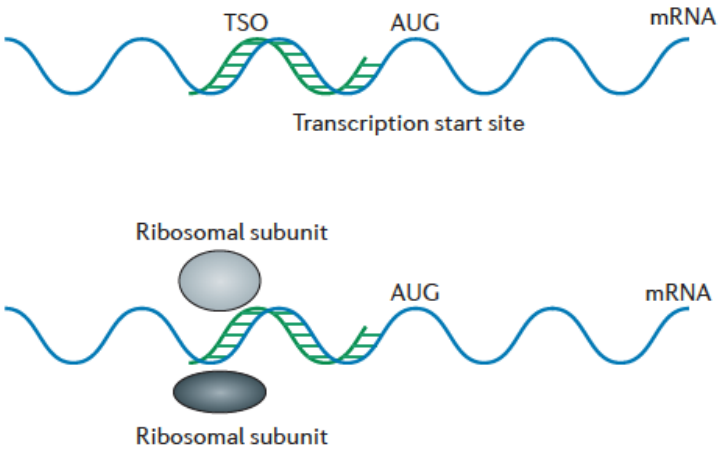

Figure 3. Mechanism of target gene silencing by antisense oligonucleotides. Translation-suppressing antisense oligonucleotides (TSOs) bind to target mRNA sequences near the translation initiation codon (AUG). The altered backbone of the synthetic TSO interferes with ribosomal binding to the mRNA thereby suppressing translation (Kole et al., 2012).

silences expression of the target gene. The capacity for nucleic acid hybridization is conferred by the distinctive structure shared by all antisense oligonucleotide classes: 10 to 20 natural DNA bases connected by modified backbone linkages (Geller, 2005). The length of antisense oligonucleotides allows for high binding specificity, since any sequence greater than 10-20 base pairs is unlikely to repeat in a bacterial genome. Additionally, their modified backbone linkages protect against degradation by cellular enzymes (Mansoor and Melendez, 2008). This potent combination of specificity and stability has rendered antisense oligonucleotides powerful tools for the silencing of specific gene expression.

There are approximately a dozen classes of synthetic antisense compounds that have been tested thus far. All use the same bases as DNA or RNA, but differ in the structure of the linkages between bases. Currently three of these classes are the main focus of development for antibacterial compounds; locked nucleic acids, peptide nucleic acids, and phosphorodiamidate morpholino oligomers.

Locked Nucleic Acids

The first major class of third generation antisense oligomers is the locked nucleic acids (LNAs). LNAs are DNA analogues characterized by a rigid structure that favors duplex formation with nucleic acids (Singh et al., 1998). LNAs' inflexible conformations are due to the ribose ring being 'locked' into a C3'-*endo*/N-type conformation, a result of their backbones' methylene linkage between O2' and C4' on the sugar group (Figure 4). This methylene bridge forces the LNA to remain in a single RNA-like conformation, thereby minimizing the loss of entropy that occurs upon hybridization with the target mRNA molecule (Campbell and Wengel, 2011; Veedu and Wengel, 2009; Vester and Wengel, 2004). This locked shape also enables LNA-DNA or LNA-RNA duplexes to experience increased base-stacking interactions relative to unpaired nucleic acids, rendering the synthetic hybridization reactions enthalpically favorable (Singh et al., 1998). The enthalpic and entropic benefits deriving from LNA hybridization significantly stabilize the bound target sequence, raising the melting temperature on average 4-10 °C per LNA monomer (Campbell and Wengel, 2011). Melting temperature studies have also shown LNA base pairing to be stringently specific; a single mismatch in an LNA/RNA or LNA/DNA duplex decreases the denaturation temperature by 17-22 °C, whereas a DNA/DNA mismatch

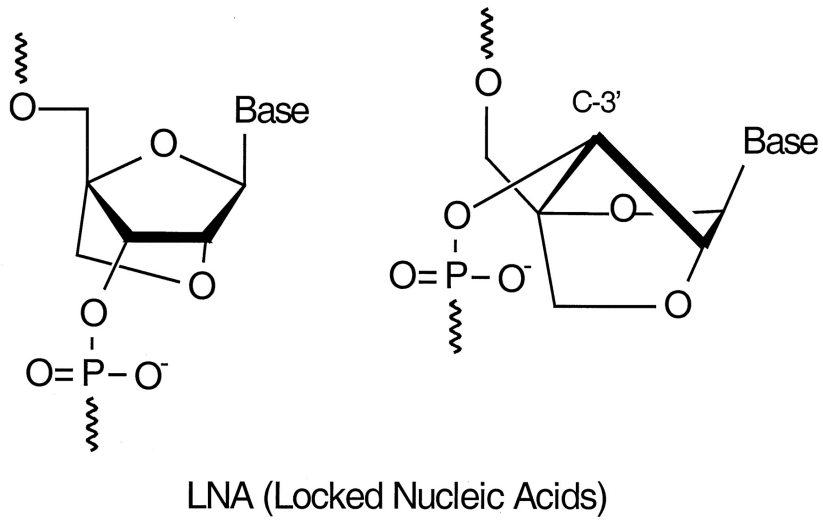

Figure 4. **Molecular structure of locked nucleic acid (LNA) antisense oligomers**. The "Base" in both schematics denotes placement of an organic nucleotide base: adenine, cytosine, guanine, or thymine. The approximately canonical A-type helix structure of LNA-RNA hybrids has been confirmed through NMR spectroscopy studies with a mix of LNA-mers (Petersen et al., 2002; Vester and Wengel, 2004; Wahlestedt et al. 2000).

lowers the denaturation temperature by 17-22 °C, whereas a DNA/DNA mismatch lowers the denaturation point by 4-16 °C (Campbell and Wengel, 2011; Vester and Wengel, 2004). Despite the strong affinity and stability of LNA target hybridization, these antisense oligonucleotides present some difficulty in implementation. Their extreme affinity can be a weak point: LNA oligonucleotides must be designed to avoid large self-complementary segments to prevent intra-molecular binding, and could readily bind non-targeted mRNA to cause unexpected regulatory effects (Jepsen et. al, 2004). Reliable, efficient delivery of LNA into cells has presented additional challenges for the use of these antisense oligonucleotides. Even LNA/DNA hybrids conjugated with cell-penetrating peptides have shown minimal success of cell penetration in microscopy localization studies (Jepsen et al., 2004, Traglia et al. 2012).

Peptide Nucleic Acids

Contrasting with LNAs, peptide nucleic acids (PNAs) are a third generation antisense oligonucleotide class distinguished by backbones with neutral charge. Unlike LNAs and organic nucleic acids, PNAs connect their purine and pyrimidine bases through acyclic, achiral methylene carbonyl linkages (Fig. 5) (Nielsen and Egholm, 1999; Shakeel et al., 2006). Since they lack the sugar moieties and phosphate groups characterizing organic genetic material, PNAs possess chemical character much more like peptides than nucleic acids. However, PNAs readily adhere to nucleic acid target molecules through stably adopting A-form conformations in duplex (Nielsen and Egholm, 1999). This stability and favorability for binding is evidenced by X-ray crystallography and the high affinity that PNAs exhibit for genetic material. Like LNAs, a base-pairing mismatch between a PNA compound and the target nucleotide sequence is more unfavorable than a mismatch in a nucleic acid duplex. Even a single mismatch in a PNA/RNA or PNA/DNA duplex can lower the denaturation temperature of the hybrid molecule by 8-20 °C, compared to a 4-16 °C drop in native nucleic acid duplexes as mentioned previously (Shakeel et al., 2006). This high affinity and multiple other advantages for PNA binding can be attributed at least in part to the neutrality of their methylene carbonyl “pseudo peptide” backbones. The absence of charge repulsion between RNA and PNA compounds allows the AO to bind more strongly than native nucleic acid complexes (Nielsen and Egholm, 1999). Inherent neutrality also enables PNAs to efficiently hybridize in a variety of ionic conditions since positive salt ions are not required to counteract the usual inter-strand negative repulsion between nucleic acid duplexes (Nielsen and Egholm, 1999;

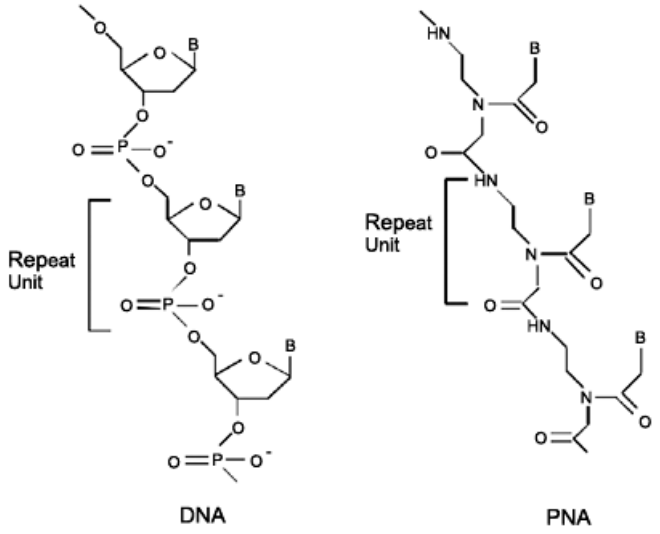

Figure 5. PNA versus DNA Scaffolds Molecular structure of a peptide nucleic acid (PNA) antisense oligomer compared to an organic DNA oligomer. The "B" in both schematics denotes placement of an organic nucleotide base: adenine, cytosine, guanine, or thymine. (Wang & Xu, 2004).

Shakeel et al., 2006). PNAs are also stable across a wide range of pH values and temperatures since the neutral compounds won't depurinate in acidic conditions like DNA (Uhlmann et al., 1998). But the peptide backbone of PNAs has also prevented their wider use as an *in vivo* tool for therapeutics and research. Namely, PNAs exhibit poor efficiency of intracellular penetration (Rathee et al., 2012, Koppelhus & Nielsen, 2003). Since cationic charge facilitates an external molecule's passage through the negative bacterial membrane, various studies have investigated incorporating positive residues or peptide chains into PNA compounds (Good et al., 2001, Rathee et al., 2012). These techniques have yielded limited success with some contradictory findings between studies. Although Good et al. reported increased inhibition of *Escherichia coli* growth following conjugation of a PNA with an amphipathic peptide, efficacies of carrier peptides exhibit a species-dependent effect (Good et al. 2001, Hatamoto et al. 2010). The large variation of penetration between bacterial species suggests the need for further investigation of peptide tagged PNAs to better

understand their intracellular delivery capacity. The conflicting data on PNAs with and without peptide side chains have demonstrated cellular penetration to constitute a serious weakness in their application (Rathee et al., 2012, Hatamoto et al. 2010).

Phosphorodiamidate Morpholino Oligomers, With or Without Polypeptide Tags

Like PNAs, phosphorodiamidate morpholino oligomers (PMOs) are also DNA mimics with uncharged backbone structures that provide exceptional stability in diverse ionic, pH, temperature conditions (Heasman, 2002). However, their novel backbone readily sets PMOs apart from LNA and PNA competitors. The PMO class is distinguished by the replacement of organic phosphodiester bonds with phosphorodiamidate linkages between nucleobases, and employment of a six-membered morpholino ring to fill the position occupied by deoxyribose in DNA (Fig. 6). These design elements were chosen because the reaction converting ribose to morpholinos is relatively simple and inexpensive, paving the way for convenience of mass synthesis (Summerton and Weller, 1997). PMOs' backbone structure also protects the molecule against degradation by cellular nucleases and limits the binding affinity of PMOs to nucleic acids (Moulton and Yan, 2003; Heasman, 2001). Although exhibiting substantially better specificity than DNA in intracellular and extracellular thermal melt studies, PMOs' target binding affinity does not exceed that of native RNA (Moulton and Yan, 2008; Summerton et al. 1997, Stein et al. 1997). This prevents the intra-molecular binding problems that compromise LNA action, while still allowing PMOs to exert their effects by hybridizing with single-stranded loops occurring in the mostly double-stranded mRNA secondary structures (Moulton, J., and Yan, Y., 2008).

PMOs also readily surmount the biggest obstacles for PNA action: crossing bacterial membranes to enter the target cell (Moulton et al., 2004; Geller et al., 2003). Although their neutral backbone might be expected to cause bacterial entry difficulties, tagging PMOs with amphipathic peptides to create peptide-PMOs (PPMOs) has already proven a broadly successful technique *in vivo* and *in vitro* for penetrating the membranes of pathogens including *Escherichia coli, Acinetobacter baumannii, Salmonella enterica,* and *Burkholderia cepacia* among others (Fig. 6). The mechanism by which PPMOs enter target cells remains incompletely understood, but current literature demonstrates that tagging PMOs with amphipathic peptides increases antimicrobial potency by orders of magnitude (Mellbye et al., 2009; Geller et al., 2013; Tilley et al.. 2006; Greenberg et al., 2010). Initial investigations of PPMOs' cellular delivery suggest that penetration efficiency varies with the structural compositions of both the peptide tag and the target membrane (Henriques et al., 2006; Mellbye et al., 2009; Yeaman et al., 2003; Tilley et el., 2006; Geller et al., 2013). This postulation is supported by studies confirming that PMOs with peptide tags containing the cationic-hydrophobic-cationic residue motif induce the greatest improvements in antimicrobial potency in *E. coli* but not in other Gram-negative species (Tilley et al., 2006; Mellbye et al., 2009; Greenberg et al., 2010). Further refinements in the optimal composition and arrangement of PPMO peptide sequence motifs are being investigated as viable approaches to improve PPMO antimicrobial effects in various bacterial strains.

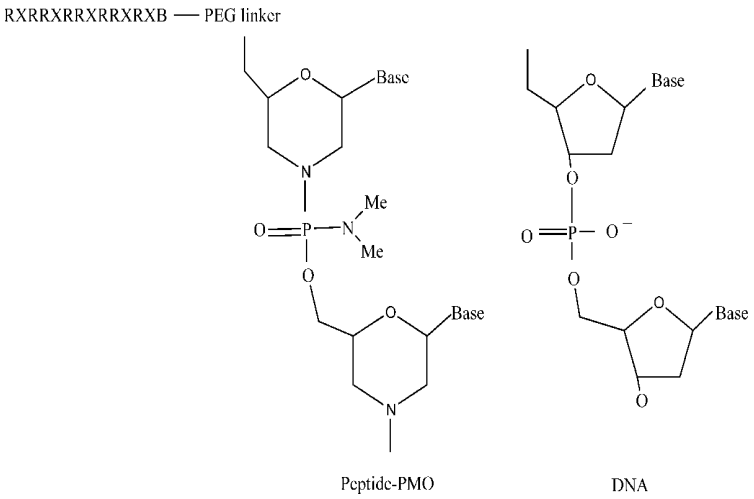

Figure 6. PPMO versus DNA Scaffolds Molecular structure of a polypeptide phosphorodiamidate morpholino oligomer (PPMO) side by side with a native DNA oligomer. The ampipathic peptide tag in this example consists of alternating arginine (R), 6-aminohexanoic acid (X), B-alanine (B) residues. However, multitudinous combinations of cationic and hydrophobic residues have been used with varying degrees of success. (Geller, unpublished).

Development of Peptide-Phosphorodiamidate Morpholino Oligomers As Commercial Antibiotics

Rational drug design for any disease is founded on the development of therapeutics with exclusive affinity for targets possessing established roles in the disease state. Subsequently, PPMOs' specific hybridization to bacterial mRNA has rendered this antisense oligonucleotide class a fertile area for rational antibiotic design. The stringent affinity of PPMOs for their gene targets is demonstrated by the significant decrease in antisense activity resulting from even a single mismatch in the complementary target sequence (Greenberg et al., 2010; Moulton and Yan, 2008). By contrast, PPMOs with complete sequence homology to their target regions have shown potent gene inhibition effects at concentrations as low as 100 nM both *in vitro* and *in vivo* (Geller et al. 2013, Summerton et al. 1997). This exquisite specificity for

their respective mRNA target regions allows any and all known bacterial sequences to constitute potent, putative ligands for antimicrobial PPMOs.

The diversity of potential PPMO drug targets is further aided by the flexibility of design afforded by the artificial backbone of these compounds. The placement of varying nucleobases along the phosphorodiamidate scaffold does not alter the primary configuration of PPMOs. Subsequently, the PPMO backbone serves as a customizable platform for nucleobase sequence modifications to suit a particular target sequence. The consistency of PPMOs' general structure across differing gene targets enables compound variants to be produced on a mass scale by commercial automated synthesis in a matter of weeks (Moulton and Yan, 2008; Mansoor and Melendez, 2008). Additionally, the stability and recyclability of the morpholino subunit predominantly comprising the PPMO backbone reduces production costs by at least an order of a magnitude relative to corresponding DNA analogs (Summerton and Weller, 1997).

Taken together, PPMOs exhibit a structural chemistry that is uniquely adaptable, durable, and economical for drug design. Thus there is no surprise that the partner institution for our research, Sarepta Therapeutics, has built their company on the premise of PPMO-mediated, RNA-based disease therapies. Collaborating with the synthetic chemists of Sarepta's laboratories has enabled us to affordably produce the panoply of PPMOs we design against multitudinous gene targets in various pathogens.

Designing Antibiotic PPMOs for Inhibition of Bacterial Gene Targets

There exist two major considerations for the creation and positioning of PPMOs on their mRNA target sequences: (a) prediction of mRNA secondary structures and subsequent identification of preferred local structures in the sequence; (b) size and proximity of the PPMO binding site to the translational start codon. To a lesser degree, GC content and the presence of activity enhancing motifs could also play a part in PPMO design (Chan et al. 2006; Deere et al., 2004). However, secondary structure of mRNA is widely accepted to be the critical element for successful PPMO design (Geller, 2005; Moulton and Yan, 2008; Kretschmer-Kazemi Far et al., 2001). Since PPMOs hybridize with lower affinity for RNA than RNA itself, effective PPMO design necessitates accurate prediction of regions in the target mRNA where PPMOs are likely to bind. The public domain program *m*fold is used in our lab and the scientific community at large to estimate all possible optimal structures of a particular mRNA sequence (Chan et al., 2006; Mansoor and Melendez, 2008). The core algorithm of *m*fold uses overall minimum free energy as the predictive factor of mRNA secondary structure. Although this automated, theoretical approach to structural calculations leaves a large margin for variations and inaccuracies, *m*fold is indispensable for predicting the position of local mRNA structures accessible for PPMO hybridization. Specifically, PPMO binding most favorably occurs where mRNA is single-stranded: regions near the terminal end, internal single-strand bulges of 10 nucleotides or more, joint sequences, and hairpin stem-loops (Kretschmer-Kazemi Far et al., 2001). The importance of these single-stranded structures was demonstrated in an antisense positioning paper by Deere et al.

examining PMO inhibition of luciferase in *E. coli*. The analysis of Deere et al. showed a significant negative correlation between PMO inhibition and internal double-stranded regions within the mRNA (Deere et al., 2004). Shifting the PMO target mRNA region slightly upstream or downstream of the unfavorable secondary structure allowed the PMO to effectively inhibit luciferase expression. Overall, identification of favorable mRNA structures crucially informs PPMO design to target only those complementary sequences optimal for interaction with the antisense oligonucleotide.

Following isolation of the target mRNA regions most available for PPMO hybridization, PPMO design must next take into account all possible binding sites' proximities to the translational start codon AUG. The initiation codon region is well established in current literature as the most effective PPMO target (Geller et al., 2005; Mansoor and Melendez, 2008). However, contradictory experimental findings prevent any conclusions on the benefits of targeting PPMOs to bases upstream versus downstream versus overlapping the AUG codon (Moulton and Yan, 2008; Chan et al., 2006). The selection of target bases flanking the start codon is also nuanced by considerations of the optimal PPMO size. Antisense oligomers must have enough bases to favorably bind unique sequences in the bacterial genome without nonspecific effects. Simultaneously, they must minimize their length to prevent potential intra-molecular binding and cellular delivery complications. Although requiring ~16 bases for inhibition of gene expression in eukaryotes, PPMOs between 9-12 bases in length have shown broad success in inhibition of bacterial translation (Summerton, 1999; Mellbye et al., 2009; Geller et al., 2013; Tilley et al.. 2006; Greenberg et al., 2010).

Importantly, experimental analyses have demonstrated these short PPMOs to silence target gene expression with exquisite specificity. In tandem with Deere et al.'s work on PMO specificity, our lab produced some of the foundational data revealing PPMOs to exert direct, dose-dependent inhibitory effects on their target genes' activity in the bacterial cell milieu. Geller et al. treated *E. coli* with varying dosages of PPMOs designed against *myc* and *lacI*. The *myc* target was chosen for its dose-dependent inhibition of luciferase, enabling direct measurement of PPMO dose response via the proportional increase in luciferase expression due to silencing of *myc*. Similarly, our lab examined inhibition of the *lacI* repressor for the positive B-galactosidase signal that PPMO-mediated *lacI* silencing would induce. Proportional, increases in luciferase and B-galactosidase production following treatment by myc-PPMO and lacI-PPMO respectively, and not the scrambled PPMO control, strongly support the effects of our PPMO treatments to be genetically specific in *E. coli* (Geller et al., 2003). Similar findings were published in a 2006 study by Tilley et al., showing that PPMOs targeted to the start codon region of the *Salmonella enterica* luciferase gene *luc* consistently inhibit luciferase expression in a dose-dependent manner (Tilley et al., 2006). Unfortunately, the novelty of PPMO compounds and the difficulty of their synthesis for small research labs has sharply limited the collection of PPMO bacterial gene specificity data outside our laboratory group and collaborators.

PPMOs as Antibiotics Through Inhibition of Essential Gene Targets *in vitro*

Current literature has thoroughly illustrated the potency of PPMOs' antimicrobial capacity against various Gram-negative bacteria, pathogens and non-pathogens alike. Mellbye et al.'s 2009 study demonstrated effective wild-type *E. coli* K-12 W3110 growth inhibition by an assortment of differently tagged PPMOs targeted to the same 11-base sequence in the start codon region of the acyl carrier protein gene *acpP*. Acyl carrier protein is a universal, highly conserved shuttle for fatty acid intermediates during their synthesis and metabolism. Due to *acpP*'s central role during fatty acid biosynthesis, expression of this gene is essential for bacterial survival (Martinez et al., 2010). By targeting this essential gene for binding and thereby translational arrest, 6 different AcpP-PPMOs prevented *E. coli* growth in rich media at clinically relevant minimum inhibitory concentrations (MICs) despite the variations in effectiveness correlating with their individual peptide tags' residue composition (Mellbye et al., 2009).

Tilley et al. performed a similar PPMO experiment targeting *acpP* for silencing in enteropathogenic *E. coli* E2348/69 as well as the pathogenic *Salmonella enterica* serovar Typhimurium, reasoning *acpP*'s demonstrably critical role in *E. coli* viability would extend to additional Gram-negative species. As in Mellbye et al.'s 2009 study, AcpP-PPMOs were designed to bind a single sequence immediately next to the *acpP* start codon but differed in the residue composition of their peptide tags. Dose-response analyses of the AcpP-PPMOs in each pathogen revealed clinically relevant treatment concentrations of 5.3 uM and below successfully reduced bacterial colony forming units (CFUs) by 50% compared to the control. Interestingly, similar

antibacterial potency was achieved with even lower PPMO concentrations for *E. coli* E2348/69 in tissue culture. Tilley et al. infected Caco-2 intestinal epithelial cells with *E. coli* 2348/69 and immediately treated with PPMO doses ranging from 0.1-10 uM. Viable cell counts taken 24 hours following infection and treatment showed PPMO treatment to reduce *E. coli* CFU/mL counts by 50% at concentrations as low as 3.0 uM. Their study is the first to provide important evidence of PPMO bactericidal potency against *Salmonella* in culture, and was verified by a subsequent paper from Mitev et al. evaluating AcpP-PPMO inhibition of *Salmonella* growth in intracellular culture (Tilley et al., 2006; Mitev et al., 2009). These studies' success inhibiting the growth of two common, pathogenic bacterial strains lends strong support to the premise of PPMO use as antibiotic compounds.

The medical relevance of PPMOs has been further strengthened by Greenberg et al.'s demonstration of PPMO's success inhibiting a panel of *Burkholderia cepacia* clinical isolate strains. Like the Mellbye et al. and Tilley et al. experiments, the Greenberg research team used individually tagged PPMOs to target the start codon region of the *acpP*. However, Greenberg et al.'s PPMO targeted different sequences either immediately downstream of or spanning the start codon of *acpP*. Despite their different base-sequence targets, both PPMOs tagged with the membrane-penetrating peptide $(RFF)_3RXB$ were bactericidal to *B. cepacia* cultures grown in rich culture and demonstrated clinically relevant MICs. The absence of effect in the third PPMO was attributed to its tag peptide $(RXR)_4XB$, which efficiently promotes entry in *E. coli* but appears unsuitable for *B. cepacia* penetration. These pure culture MIC measurements were complemented with neutrophil killing assays in Greenberg et

al.'s study. The killing assays measured bactericidal effects of PPMOs added to human neutrophil tissue cultures incubated with the clinical isolate *Burkholderia multivorans*. An approximately 3-log reduction in bacterial CFUs was observed in the neutrophil cultures treated with AcpP-PPMO, compared to the untreated control tissue. The decreased CFU count in the treated culture indicates PPMOs not only inhibit bacterial growth independently, but also enhance neutrophil-mediated bacterial killing (Greenberg et al, 2010). These results are especially significant due to *B. cepacia*'s role as an opportunistic pathogen causing chronic infections in cystic fibrosis patients. Many *B. cepacia* strains isolated from such patients are intrinsically antibiotic resistant. Even drugs of last resort are only able to inhibit 20-40% all *B. cepacia* cystic fibrosis isolates (Zhou et al., 2007). This context of prevalent, intense resistance underscores the antibiotic promise PPMOs hold as potent inhibitors of microbial growth, even for such resistant organisms as *B. cepacia*.

Acinetobacter baumannii is another pathogen characterized by highly resistant infections, often causing significant morbidity and mortality due to the absence of successful treatments (Peleg et al., 2008). In conjunction with collaborators in the Greenberg team, our lab successfully inhibited the growth in 6 *Acinetobacter* strains of varying antibiotic resistances by treating them with PPMOs targeted to varying base sequences in 3 putatively essential genes. The three gene targets were *acpP*, the acyl carrier protein target proving potent for inhibition of other bacterial species, *ftsZ*, encoding the cell division regulatory protein FtsZ, and *rpsJ*, a ribosomal subunit protein gene. These genes were chosen since each possessed homologs identified as essential in the closely related species *Acinetobacter baylyi* (de Bernardinis et al.,

2008). Through counting pure culture CFUs/mL following 24 hour PPMO treatment, PPMOs targeted to base sequences directly upstream of the *acpP* start codon were shown to be the most potent growth inhibitors across all 5 *A. baumannii* strains as well as the opportunistic pathogen *A. lwoffii* 17976 (Geller et al., 2013). Despite the high antbiotic resistances integral to the chosen *A. baumannii* strains, PPMOs binding upstream of the *acpP* AUG were demonstrated consistent, dose-dependent bactericide at clinically relevant MICs. The AcpP-PPMOs' ability to reduce bacterial viability by orders of magnitude even in *A. baumannii* strains resistant to drugs of last resort suggest these oligomers to be a potential new therapeutic for last-line treatment of resistant infections.

Despite the effective inhibition PPMOs have exhibited across a broad range of Gram-negative bacteria species *in vitro*, Gram-positive bacteria remain mostly untested by PPMOs. Peptide-PNAs have shown up to 100% growth inhibition by targeting the essential genes *gyrA*, *fmhB*, and *hmrB* of *Staphylococcus aureus* in pure culture, but few similar investigations with PPMOs have yet been performed (Geller et al., 2005). The one exception is 2012 study by Panchal et al. inhibiting *B. anthracis* proliferation with PPMOs targeted to the acyl carrier protein gene and gyrase A gene. The cessation of *Bacillus anthracis* growth *in vitro* and *in vivo* suggests essential gene PPMOs could be successful inhibitors in Gram-positive as well as Gram-negative pathogens (Panchal et al., 2012). PPMOs have set a precedent of successful inhibition in *E. coli*, *S. enterica*, *B. cepacia*, and *A. baumanii*. Future investigations should include targeting the essential genes of similarly significant Gram-positive pathogens to broaden the scope of PPMO applicability as a therapeutic.

PPMOs as Antibiotics Through Inhibition of Essential Gene Targets *in vivo*

PPMOs have been tested *in vivo* using animal models of infection. Mellbye et al. tested their AcpP-PPMOs on mice infected with the wild-type *E. coli* W3110 strain they had used for MIC assays in pure cell culture. The Mellbye group treated the infected mice by injecting varying doses of the four PPMOs that exhibited the greatest potency *in vitro*. They were then able to determine PPMO effects by measuring CFU/mL in blood samples taken from the mice over the first 12 hours posttreatment. This experimental setup allowed Mellbye et al. to determine that PPMO dosages as low as 30 ug were able to reduce blood bacteria levels by 98% compared to the scramble-PPMO controls, while treatment with 30 ug of ampicillin did not cause a significant effect. However, increasing the rate of survival in mice required similarly high concentrations of 100-300 ug for both ampicillin and PPMO. Mellbye et al.'s data confirm the results from an earlier, nearly identical experiment by Tilley et al. examining treatment of intraperitoneal *E. coli* W3110 infections with AcpP-PPMOs injections in a mouse model. Although Tilley et al. used different peptide tags than Mellbye et al. on their tested PPMOs, the two studies' *acpP* mRNA target sequence and protocols for data collection were the same. Unsurprisingly, their results were the same as well: Tilley et al. also reported orders of magnitude reduction in blood CFU/mL counts following PPMO treatment as well as enhanced survival rates with PPMO dosages of 100 ug or above. These reproducible results provide solid evidence that PPMOs can significantly inhibit *E. coli* infections when administered at dosage levels comparable to standard antibiotic regimens (Mellbye et al., 2009).

Greenberg et al. also chose the mouse peritonitis model for their *Burkholderia cepacia* AcpP-PPMO *in vitro* study, but measured efficacy in terms of survival at day 30 and histopathological phenotypes as well as blood CFU counts. Mice infected with *B. multivorans* and treated with 200 ug of AcpP-PPMO showed a 16 fold drop in blood bacteria counts overall when compared to the control. These bacterial counts significantly predicted mortality risk: mice whose bacterial load decreased due to their 200 ug treatment with the AcpP-PPMO had 2-fold increased survival compared to the scrambled PPMO control. Histopathology of the mouse spleens also correlated with the treatment groups, showing severe splenitis and necrotic lesions in mice dosed with scrambled controls while the PPMO-treated group manifested almost no symptoms. Greenberg et al.'s multifaceted approach to AcpP-PPMO assessment in an early stage clinical model constitutes thorough support for the relevancy of these gene-specific inhibitors for future therapeutic development (Greenberg et al. 2010).

Most recently, AcpP-PPMOs have been tested *in vivo* against *Acinetobacter lwoffii* and *Acinetobacter baumannii* by our laboratory and collaborators through use of a mouse pneumonia model. Geller et al. infected mice intranasally with *A. lwoffii* and then treated with various AcpP-PPMO doses at 5 minutes, 18 hours, and daily for 6 days following initial infection. Effectiveness of *A. lwoffii* inhibition was measured by mouse survival and CFUs of *A. lwoffii* detected in the lungs 24 hours after PPMO treatment. Mice treated with the AcpP-PPMO showed dose-dependent increases in survival, and survived significantly longer than mice treated with the scrambled PPMO control at concentrations of 5 ug or greater. Concentration dependent effects on CFU loads remain unknown since bacterial counts were taken solely from mice

treated with a single 50-ug dose of PPMO. However, this 50 ug dose was observed to reduce CFU per gram of lung by 16-fold compared with the scrambled PPMO treatment. A similar mouse pneumonia model was performed by Geller et al. to determine the potency of *A. baumannii* inhibition *in vivo* by an AcpP-PPMO. Specifically, mice intranasally infected with multidrug-resistant *A. baumannii* AYE were assessed for morbidity and mortality over the course of 1 week following intranasal treatment with an AcpP-PPMO. All mice treated with the PPMO exhibited reduced morbidity, manifested by higher weights and body temperatures, compared to the scramble-PPMO treated control. More importantly, AcpP-PPMO treated mice uniformly survived the duration of the pneumonia experiment while scrambled-PPMO controls succumbed to their infection usually within 24 hours (Geller et al., 2013). The survival advantage conferred by AcpP-PPMO treatment was statistically significant, and further strengthens the case for PPMOs as antibiotics ready to be developed in increasingly relevant clinical models.

Safety Considerations for PPMO Development

The notable successes of PPMO antibiotics in the laboratory have been complemented with examinations of their safety profile in rodent *in vivo* models. Despite the appeal of their bactericidal toxicity, considerations for safety of practical use mandate confirmation that PPMO toxicity is specific to their bacterial targets. To this end, several pharmacokinetic studies have explored the biodistribution and toxicity of PPMOs in mice and rats (Adams et al., 2007; Stein et al., 2008).. Evolution of bacterial resistance to PPMOs constitutes the other major safety consideration for the development of these compounds as novel antibiotics.

Putatively, the gene-specific mechanism of PPMO action will limit bacterial resistance since changing these gene sequences would likely incur severe genetic damage to the pathogen. However, the recency of PPMOs' application as antibiotics has necessarily limited the available knowledge in this area of PPMO safety.

Toxicity of PPMOs

Assessment of PPMO toxicity has most commonly been performed in rodent *in vivo* models over short experimental periods of highly concentrated PPMO treatments. Adams' group pioneered this field of study with their 2007 paper, examining PPMO aggregation and pathological effects in healthy rats treated with 15-150 mg/kg morpholino doses for 5 days. Their research revealed PPMOs to primarily accumulate in the kidney and liver, with lower concentrations recorded in the spleen, heart, lungs, and even the brain (Amantana et al., 2007). These results were corroborated by data gathered in Stein et al.'s 2008 study on antiviral PPMOs: Stein's group demonstrated PPMO tissue levels in mice were 30 times greater in the liver and 10 times greater in the spleen than in the brain (Stein et al., 2008). Despite the broad bodily distribution of PPMOs in these experiments, significantly deleterious effects on organ integrity or function were never observed at in the clinical dose range of 10-40 mg/kg (Amantana et al., 2007; Stein et al., 2008). Similarly, neither study found PPMO treatment to harmfully impact animal behavior or appearance until at concentrations greater than these doses. In Amantana et al.'s toxicity study, PPMO treatments were not lethal to rats until concentrated as high as 210 mg/kg. Stein's research group only examined PPMO toxicity at the low, clinically approximate dose of 10 mg/kg and thus did not observe any morbidities (Stein et al., 2008).

Additionally, preliminary data on the toxicity of PMOs without their conjugated peptides indicates that the compounds have favorable safety profiles in dogs and humans. However, the exclusion of the PPMO peptide portion in these ongoing studies limits their applicability for explorations of PPMO safety profiles. These *in vivo* canine and human models are also rendered less relevant due to the targeting of test PMOs to eukaryotic gene sequences for the treatment of Duchenne muscular dystrophy (Moulton and Moulton, 2010; Malerba et al., 2011). Regardless, the patterns emerging in the novel field of PPMO toxicity show these compounds display minimal toxicity at clinically relevant treatment doses in *in vivo* invertebrate models.

Resistance to PPMOs

By contrast, PPMO resistance mechanisms have primarily been studied in *in vitro* systems. The possibility of spontaneous PPMO insensitivity is a particularly pressing concern for the research community, since this rapid development of resistance would reduce PPMO advantages compared to classical antibiotics. Puckett et al. studied this phenomenon through use of multi-generational *E. coli* passaging in rich media supplemented with low doses of three AcpP-PPMOs. Two of the three PPMOs tested never induced significant bacterial resistance, and mutants resistant to the third PPMO were generated at rates similar to spontaneous mutation for individual *E. coli* genes. This absent or relatively low rate of resistance development suggests that few genes are capable of producing a PPMO-resistant phenotype. The few PPMO-resistant mutants obtained were sensitive to general small-molecule antibiotic treatment, demonstrating the bacterial resistance to be PPMO-specific. This

specificity was explained by the identity of the gene responsible for the resistance phenotype; only *E. coli* with a missense mutation in *sbmA* were resistant to AcpP-PPMO treatment. The gene *sbmA* encodes an active transporter for peptide antibiotic substrates. Subsequently, its loss may have resulted in PPMOs being unable to cross the bacterial membrane. The causative effect of this gene's deletion suggests PPMO resistance to be related more to the peptide than the phosphorodiamidate morpholino oligomer itself (Puckett et al., 2012).

These data partially corroborate the previous paradigm of PPMO resistance established by antiviral research. Dr. Benjamin Neuman's group at the Scripps Research Institute performed one of the earliest analyses of PPMO resistance, as described in his 2005 study on PPMOs for treatment of severe acute respiratory syndrome coronavirus (SARS-CoV). Neuman et al. serially passaged SARS-CoV 11 times in kidney epithelial cells treated with varying dosages of viral RNA-targeted PPMOs. Although 10 uM PPMO treatments inhibited viral growth in early cultures, partial resistance was observed within four viral passages. Although the research group did not directly investigate the relationship between the PMO peptide tag and resistance, they noted that no PPMO target sequence mutations were observed in any of the resistant mutant strains (Neuman et al., 2005). The lack of target sequence mutations indirectly supports PPMO resistance occurring as a result of the peptide tag, as opposed to alterations of the PPMO target mRNA region.

Only a 2008 study by Zhang et al. contradicts this prevailing theory of PMO peptide resistance. Their research on PPMO treatments of West Nile virus indicated a single-nucleotide mismatch in the PPMO target region was the source of viral

resistance. Specifically, Zhang's group created a mutant viral 5'RNA containing an A-to-G substitution at the PPMO hybridization site. Competition assays of PPMO treatment against this altered mRNA revealed a 50% drop in binding capacity, suggesting PPMOs would be rendered ineffective by this sort of mutation. However, the resistant viruses Zhang et al. obtained in their study were never sequenced. Thus, the results Zhang's group obtained from their artificial mRNA cannot be definitively extrapolated to actual instances of viral PPMO resistance (Zhang et al., 2008).

Experimental Approach

My thesis seeks to expand on the current body of knowledge about PPMO efficacy and mechanism of action. Employing the concepts that I have briefly synthesized in this introduction, my research explored the inhibitory potency of PPMOs targeted to myriad essential and antibiotic-resistance genes in a panel of Gram-negative pathogen strains. To better elucidate the applicability of PPMO antibiotic therapy, I investigated minimal inhibitory concentrations of PPMOs in rich and minimal medium against liquid bacterial cultures. These evaluations of target genes were complemented with a tissue culture toxicity study, yielding safety profile data to ensure the feasibility of my studied compounds' use in a clinical setting. Finally, my work examined the translational effects of PPMO inhibition through quantitative real-time polymerase chain reaction experiments.

CHAPTER 3 - MATERIALS AND METHODS

Peptide-Conjugated Phosphorodiamidate Morpholino Oligomers

All PPMOs were synthesized and purified at Sarepta Therapeutics (Corvallis, Oregon, USA) as described previously (Geller et al., 2003). PPMOs were received in lyophilized powder form and hydrated in MilliQ water to concentrations of approximately 3 mM before usage. The exact concentration of each hydrated PPMO stock was determined by measuring the absorbance at 260 nm using a NanoDrop 1000 spectrophotometer, and calculating using an extinction coefficient provided by Sarepta Therapeutics. All PPMOs were conjugated at the 3' end to the carboxyl end of $(RXR)_4$-XB side chain, except NG-06-0076 and 06-0078 which were conjugated at the 5' end.

Bacterial Cultures

The following strains were obtained from the American Type Culture Collection (ATCC); *E. coli* W3110, *E. coli* ATCC-70928, *E. coli* BAA-196, *E. coli* BAA-200, *E. coli* BAA-202, *A. baumannii* 17976, *A. baumannii* 17978, and *A. baumannii* AYE. *E. coli* BCT-036-NDM1 was kindly provided by Patrice Nordman (Centre Hospitalier, Universitaire de Bicentre, France). *E. coli* strains 1001728,

1101851, AI071077, and AI0707834 were generously given by Dr. J. Kamile Rasheed (Centers for Disease Control and Prevention, Atlanta, Georgia). *E. coli* CVB-1 was given by Rossolini (University of Siena, Italy). *E. coli* E2348/69 was donated by James Kaper (University of Maryland). *E. coli* NDM1-E was a gift from Susan Poutanen (Mount Sinai Hospital, Toronto), and , *E. coli* T66080, *E. coli* W40477, *E. coli* W41703, *E. coli* X2116, *E. coli* X2206 are clinical isolates provided by David Greenberg (University of Texas Southwestern Medical Center, Dallas, Texas). *E. coli* J53 (pNDM1) was a transconjugate constructed by Bruce Geller as follows: The NDM-1 gene in *K. pneumoniae* BAA-2146 (ATCC) was moved to *E. coli* J53 (E. coli Genetic Stock Center, Yale University) by conjugation. Exponential cultures growing in LB broth were mixed 1:4 (BAA-2146:J53) and incubated aerobically with gently agitation for 3 h. The mixture was diluted and spread on LB plus ampicillin (100 μg/ml) and NaN_3 (100 μg/ml), and the plates were incubated 18 h at 37°C. The NDM-1 gene in the transconjugate was verified by PCR (denature 95°C, anneal 48°C, polymerize 72°C, for 30 cycles) using these primers: 5'-AAGCTGAGCACCGCATTAGC AND 5'-GTTGGTCGCCAGTTTCCATT.

Screening PPMO Targets in Rich and Minimal Media

Minimum inhibitory concentration (MIC) was measured in 96-well polystyrene microtiter plates according to the microdilution method using 100 uL cultures in Mueller-Hinton II cation-adjusted broth (Clinical and Laboratory Standards Institute, 2006). Uninoculated media and scrambled, nonsense PPMOs NG-06-0078 and NG-09-0949 were used as controls. Following dilution series treatments with various PPMOs, the culture plates were incubated overnight shaking at 37 °C in

rich Mueller Hinton II broth or MOPS minimal media prepared in accordance with the E. coli Genome Project protocol (Neidhart et al., 1974). Growth was measured by optical density at 595 nm in a TECAN microplate reader. Turbidity values of 0.100 or greater were scored as growth.

PPMO and Classical Antibiotic Combination Therapy Evaluations

The ability of PPMO to reduce the MIC of standard antibiotics was measured using the clinical microdilution method (CLSI, 2006) with the following modifications: A dilution series of PPMO with a fixed concentration of standard antibiotic was made in each column of a 96-well plate. In each successive column, half the concentration of standard antibiotic was used. Each plate contained one row without PPMO and one column without standard antibiotic.

RNA Extraction

Overnight *E. coli* AIS070834 cultures were back-diluted 10-fold in fresh MHII media and immediately given one of the following treatments in triplicate:

(1) 3 mM NDM PPMO NG-12-0105 (2) 3 mM scrambled PPMO NG-06-0949

(3) MilliQ water in a volume equivalent to NDM PPMO treatment

Aliquots were taken from each sample and placed on ice after 0.5 hours, 1 hour, 2 hours, 4 hours, 8 hours, and 24 hours of treatment. RNA was then extracted from the samples using the manufacturer's protocol accompanying the RNeasy Mini Kit with Bacterial Supplement (Qiagen, Limburg, Netherlands). After chilling on ice, each sample was combined with 2 mLs of RNAprotect Bacteria Reagent in a fresh tube, vortexed, and incubated at room temperature for 5 minutes. The incubated samples were then centrifuged at 5000 g for 10 minutes. Sample supernatant was decanted

following centrifugation, and the resultant pellets were resuspended in freshly made 1 mg/mL lysozyme (Sigma-Aldrich Co., St. Louis, MO) in 100x Tris-EDTA buffer. The resuspensions were vortexed briefly to mix, and incubated at room temperature for 5 minutes. Next, 700 uL aliquots of Qiagen Buffer RLT with B-mercaptoethanol were added to each sample resuspension. After 500 uL aliquots of 95% ethanol were gently mixed into each of the tubes, the cell lysates were transferred into RNeasy spin columns. The spin columns were centrifuged for 15 seconds at 8000 g, and then 700 uL of Qiagen Buffer RW1 was added to each column before centrifuging again for 15 seconds at 8000 g. Two rounds of 5000 g centrifugation for 15 seconds were repeated afterwards using fresh 500 uL aliquots of Qiagen Buffer RPE. The RNA was then eluted by centrifuging the spin columns with 80 uL MilliQ water for 2 minutes at 8000 g, and stored at -80 °C.

cDNA Synthesis

The concentration and purity of RNA extracts was determined using a Nanodrop 1000 spectrophotometer. cDNA was reverse transcribed from 5 ug samples of total RNA from each extract using the manufacturer's protocol accompanying the SuperScript First-Strand Synthesis System for RT-PCR (Invitrogen, Carlsbad, CA). Three replicates of each RNA extract were placed in microcentrifuge tubes and combined with 1 uL of 10 mM dNTP mix, 1 uL of oligo(dT) primers, and a quantity of DEPC H_2O that brought the total sample volume to 15 uL. RNA, water, and the primers were incubated for 5 minutes at 65 °C in a waterbath (Brinkmann-Lauda, Delran, NJ) and briefly stored on ice. 2X reaction master mixes containing proportional amounts of SuperScript buffer, 25 mM $MgCl_2$, and 0.1 M DTT were

prepared during the ice incubation of RNA samples. Subsequently, 9 uL aliquots of the reaction mix were added to each chilled sample and the tubes were placed in a 42 °C water bath for 2 minutes. Following this brief incubation, 5 uL of SuperScript II Reverse Transcriptase or DEPC water (Teknova, Hollister, CA) in place of the enzyme was added appropriately to experimental and control tubes. cDNA was synthesized for 50 minutes at 42 °C in a shaking incubator (Lab-Line Instruments, Melrose Park, IL), terminated for 15 minutes in a 70 °C waterbath, and purified with 1 uL of SuperScript RNase H for 20 minutes at 37 °C. All tubes were then placed in the refrigerator for storage until use for quantitative real-time PCR.

Quantitative Real-Time PCR

A 7500 Fast Real-Time PCR System (Applied Biosystems, Carlsbad, CA) was used to run quantitative real-time PCR for each of the triplicate cDNA samples. Two uL of each sample was combined with DEPC H_2O, Power SYBR Green PCR Master Mix (Applied Biosystems, Carlsbad, CA), as well as forward and reverse primer diluted to 100 nM to create 20 uL volume reactions as recommended by the protocol. These primers were designed and optimized by Dr. Bruce Geller. Reactions with both the gene of interest *NDM1* and the housekeeping gene *16S* were performed using an undiluted, 2 uL aliquot of cDNA. The samples were incubated at 95 °C for 5 minutes and annealed at 55 °C for 6 seconds before fluorescence was measured. Next, cDNA was extended at 58 °C for 1 minute and the process repeated for a total of 40 cycles. Following the last cycle, high resolution melting analysis was performed to assess amplicon purity. Genomic contamination in the plate or reagents was controlled

through comparisons of amplication in control wells containing master mix and primers without cDNA.

Quantitative Real-Time PCR Data Analysis

For the time course experiments measured by quantitative real-time PCR, mRNA measurements from triplicate wells were averaged to generate a mean gene expression value for each treatment time point. The relative expression of the gene of interest *NDM1* was calculated in relation to the *16S* rRNA gene using C_t values. For each time point, the average of triplicate *16S* C_t values were subtracted from the averaged triplicate *NDM1* C_t values to correct for differences in cDNA concentrations between samples. The C_t values of water treated wells at each time point were then subtracted from C_t values of target-PPMO treated and scrambled-PPMO treated wells at corresponding time points to control for variations in cDNA concentrations throughout the time course. The following equation was used to determine mRNA concentration:

Relative mRNA concentration = $2^{-\Delta\Delta Ct}$ where ΔC_t = (average $C_{tNDM1} - C_{t16S}$) and $\Delta\Delta C_t$ = (avg water C_{tNDM1} at time point X- avg treatment C_{tNDM1} at time point X)

Standard error for treatment means at each time point were calculated by dividing the standard deviation of ΔC_t between triplicates by the square root of 3. All statistical analyses of genetic data were performed using the software Microsoft Office Excel 2011 (Excel, Office 2011, Microsoft, Redmond, WA, 1987-2014).

Cell Culture

Low passage number A549 human lung epithelial cells and THP-1 human monocytes were obtained from Dr. Luiz Bermudez (Oregon State University, Corvallis, Oregon) and were cultured in F-12K media supplemented with glutamine and 10% heat-inactivated fetal bovine serum (FBS) or RPMI 1640 media supplemented with 25 mM HEPES as well as glutamine and 10% heat-inactivated bovine serum, respectively. Both cell types were cultured at 37 °C in a 5% CO_2 atmosphere incubator and media was renewed every 4 days until flasks reached 75-90% confluency (A549) or visible turbidity (THP-1).

To subculture A549 cells, F-12K media was aspirated from confluent plates and replaced with 5 mL of phosphate-buffered saline (PBS). After rocking the flask gently to thoroughly rinse, the PBS was aspirated and replaced immediately with 5 mL 1X Trypsin in EDTA. The trypsin was allowed to remain on the plate for 5 minutes at 37 °C in a 5% CO_2 incubator. Cell detachment was confirmed microscopically, and trypsin activity was quenched by the addition of 10 mL of appropriately supplemented, fresh F-12K media. The cells were then triturated and a 10 uL aliquot was isolated for cell counting. The suspension aliquot was mixed with 10 uL of 0.2% Trypan Blue and placed in a Bright-Line hemacytometer (Sigma-Aldrich Co., St. Louis, MO) to determine cell concentration. Using the hemacytometer counts, new 75 cm^2 culture flasks were seeded with approximately 2 x 10^5 A549 cells in 15 mL of fresh F-12K media.

To subculture THP-1 cells, the planktonic culture in its old medium was transferred to a sterile centrifuge tube and spun down at 600 g for 10 minutes at room temperature. After removing and discarding the media supernatant, the THP-1 cell

pellet was resuspended in 2 mLs of appropriately supplemented, fresh RPMI 1640 media. A 10 uL aliquot was then isolated for cell counting. This aliquot was mixed with 10 uL of 0.2% Trypan Blue and placed in a hemacytometer to determine cell concentration. Using the hemacytometer counts, new 75 cm^2 culture flasks were started with approximately 2 x 10^5 THP-1 cells in 15 mL of fresh RPMI 1640 media. Unless otherwise specified, all reagents were from Invitrogen, Carlsbad, CA.

Toxicity Testing

Six PPMOs (NG-11-0038, NG-11-0694, NG-11-0696, NG-12-0100, NG-12-0105, NG-13-0617) were assayed for toxicity in tissue culture using a protocol developed by Dr. Bruce Geller and our collaborator Dr. David Greenberg. A549 and THP-1 cells were cultured until approximately 50% confluent or showing hundreds of cells under the microscope, respectively. At this growth stage, A549 cells were trypsinized as described previously and THP-1 cells were transferred to a fresh culture tube. From these ready preparations, 0 hour time point measurements were taken using 100 uL aliquots of each culture combined with 25 uL aliquots of 0.2% Trypan Blue counted in a hemacytometer. After recording the quantity of live and dead cells at 0 hours, 150 uL aliquots of A549 and THP-1 cells were placed in 96-well polystyrene plates and given triplicate 10 uM treatments of the six PPMOs of interest. Treated cells were cultured at 37 °C in a 5% CO_2 incubator for 24 hours, then counted using the hemacytometer as described above. Dead cell counts in each well were subtracted from total cells to calculate the percentage of living cells per well. The percentages of living THP-1 and A549 cells for each PPMO treatment were then recorded and compared to triplicate live cell counts from the untreated control wells.

CHAPTER 4 - RESULTS

Design of New PPMOs

PPMOs were designed by Dr. Bruce Geller using an algorithm that takes into account the essetiality of the targeted gene, the theoretical folding pattern of the targeted mRNA, and the position of the start codon, as described (Deere et al., 2005). Briefly, all PPMOs were 11 bases in length and complementary to the region near the start codon. BLAST searches assured that the PPMOs were not identical to complementary regions near the start codon of other essential genes. All were conjugated at the 3'-end to $(RXR)_4XB$, except 06-0076 and 06-0078. X is 6-amino hexanoic acid, B is beta-alanine, and R is arginine.

Inhibition of Growth in Rich Media

PPMOs were screened for potency by measuring the minimal inhibitory concentration (MIC) in rich broth (Mueller-Hinton II) using a panel of strains of E. coli. The potency of each PPMO in each strain is represented by color. Red indicates the PPMO was highly effective and thereby showed a low MIC range (0.5-4 uM), blue indicates the PPMO showed some effect at a higher MIC range (8-16 uM), grey indicates the PPMO did not inhibit strain growth at any tested concentration (>16 uM). The data show that the most potent PPMOs were targeted to the mRNA of acyl carrier protein gene *acpP*, regardless of the attached peptide's structure (Fig. 7). The five tested AcpP-PPMOs were able to prevent *E. coli* growth at concentrations between 0.5 and 4 uM. The lower concentration is thought to be in a clinically relevant range for parenteral administration. The only other PPMO with similarly broad and high potency was targeted to *murA*, which is an essential gene that encodes

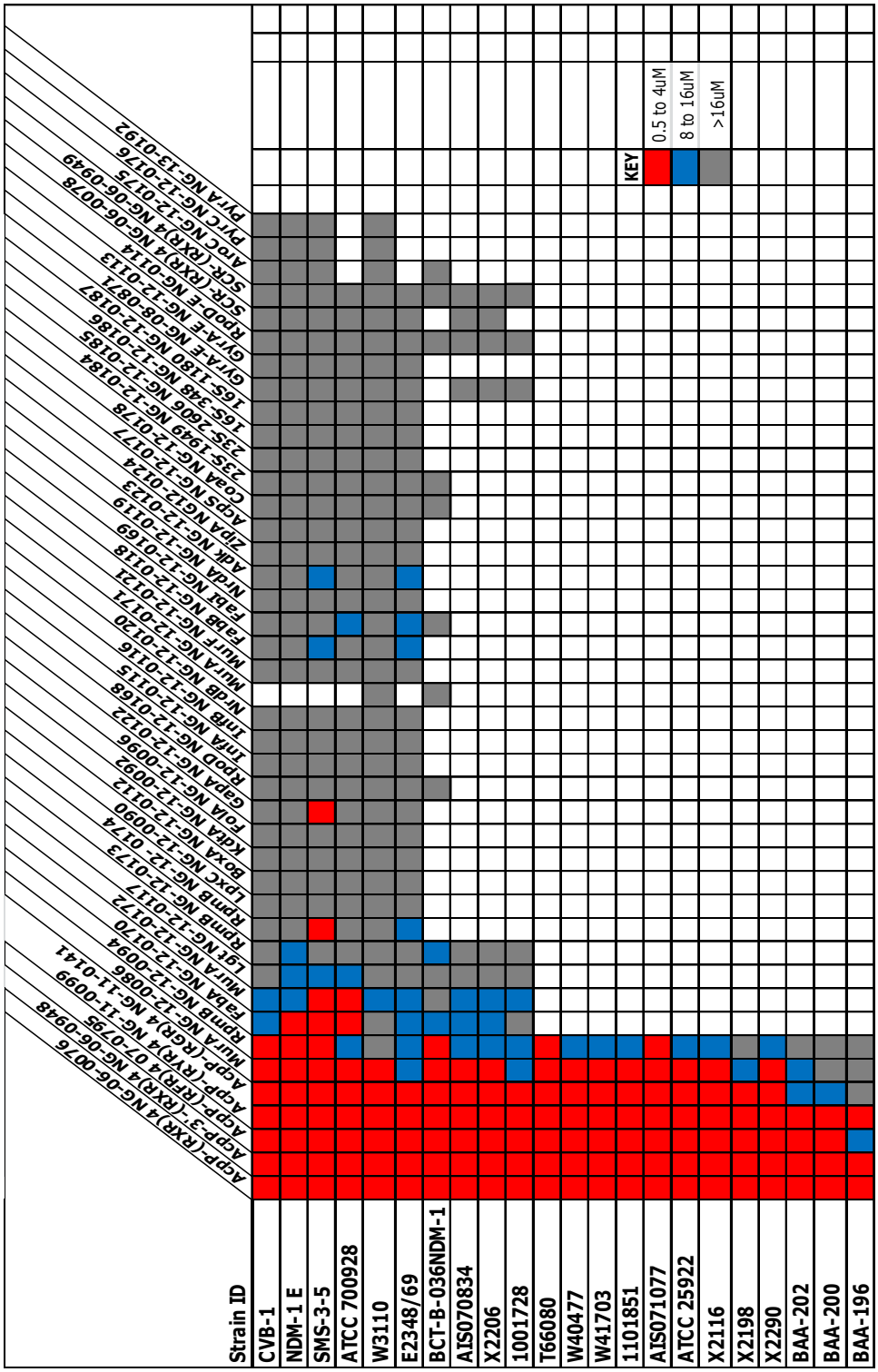

Figure 7. PPMO Targets Exhibit Conserved Efficacy Across *E. coli* Strains. Selected PPMOs targeted to essential genes in *E. coli* were tested for growth inhibitory effects by performing MIC assays in rich media on a panel of 22 *E. coli* strains collected from environmental and clinical settings.

acetylglucosamine enolpyruvyl transferase, and is required for peptidoglycan biosynthesis. Interestingly, an overwhelming majority of the essential gene targets failed to inhibit growth when treated with targeted PPMOs. This lack of inhibition could be attributed to differences in mRNA turnover or abundance of various essential genes, as well as unfavorable positioning of the PPMO on the target mRNA. Multiple PPMOs also possessed varying MICs between *E. coli* strains, exhibiting differential potency depending on bacterial context. These inter-strain inconsistencies in PPMO could reflect variations in cell wall composition that modify oligomer uptake, or differences in mRNA turnover or abundance between strains.

Inhibition of Growth in Minimal Media

PPMOs were then screened for efficacy by measuring their MIC in a defined, minimal medium. Our data show that MIC values were uniformly lower MOPS minimal media than in the rich Mueller-Hinton II broth (Fig. 8). As before, the color coded heat map indicates potency of PPMOs. Red boxes indicate the lowest effective MICs, blue boxes represent PPMOs with a medium range MIC, and grey boxes represent PPMOs without inhibitory capability below 16 uM. In addition, the pink box indicates the exceptional efficacy of the AcpP-PPMO 07-0795 against E2348/69; the MIC of this particular combination was a striking 0.03 uM. This result could indicate the positioning of AcpP-PPMO 07-0795 to most completely block expression of *acpP* relative to other AcpP-PPMOs. Similar to data from PPMO screening in rich media, oligomers targeted to the *acpP* gene demonstrated the lowest MICs. Most notably, PPMOs targeted to *Adk* and *InfA* genes prevented growth at significantly

lower concentrations in minimal medium than in rich medium. *Adk* encodes adenylate kinase, a protein responsible for reversible terminal phosphate group transfers between adenosine triphosphate (ATP) and adenosine monophosphate (AMP). Due to its key role in ATP utilization for bacterial metabolism and stress responses, *Adk* expression is crucial for stabilization of cellular energy homeostasis. *InfA* expresses the translation initiation factor IF-1 to induce the formation of peptide chains . Although *InfA*'s general purpose seems to be the stimulation of all other

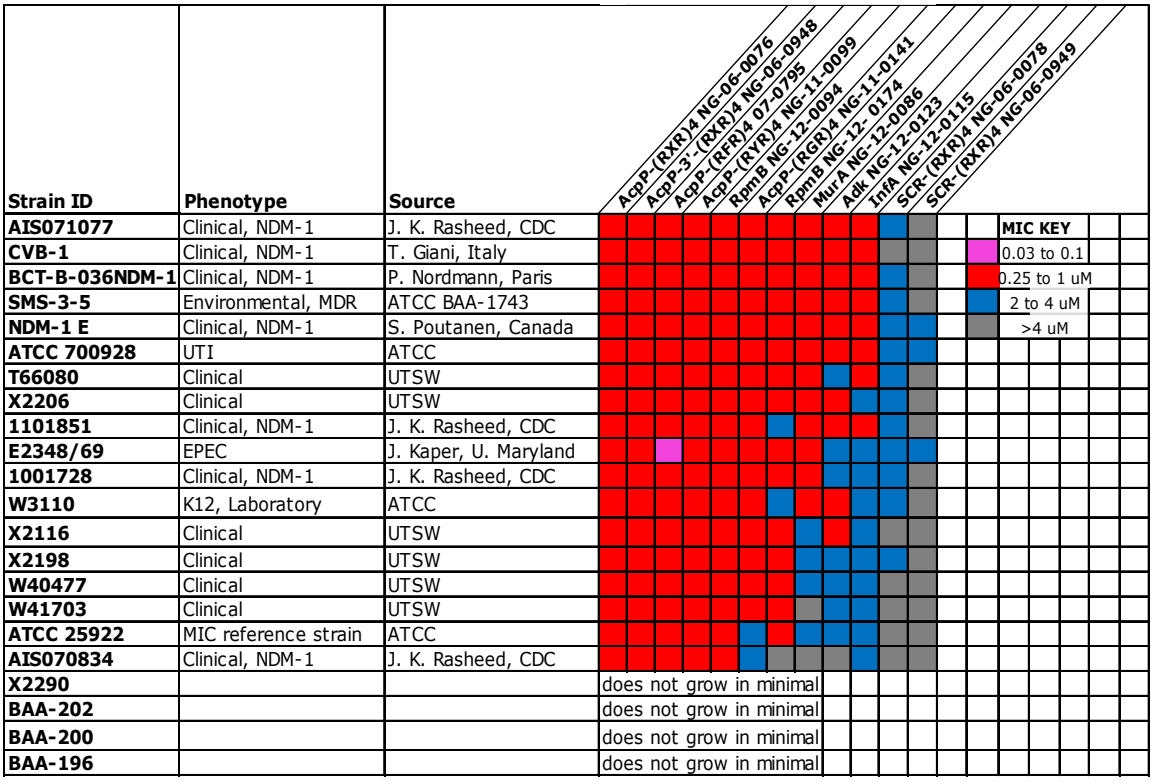

Figure 8. PPMOs Demonstrate Highest Potency in Minimal Media. *E. coli* strains treated with PPMOs targeted to essential genes were tested for growth inhibitory effects in low nutrient conditions by performing MIC assays in MOPS minimal medium. The potency of each PPMO in each strain is represented by color.

initiation factor activities, its exact function remains unknown. Regardless, both *Adk* and *InfA* synthesize proteins responsible for basic, essential bacterial functions. However, both compounds were ineffective against all tested strains in rich media in

concentrations as high as 16 uM. Their potency was only discovered once the Adk-PPMO and InfA-PPMO were applied in minimal media conditions, which lowered their MIC to the clinical range of 0.25-1 uM. The difference in these PPMOs' growth inhibition between rich and minimal media could be attributed to varying gene essentiality in different environmental context. The stresses and resources of a minimal media environment could change the importance of various genes for bacterial survival. In addition, the mRNA abundance or turnover of particular genes could become critical in the challenging context of minimal nutrients.

Silencing of Antibiotic Resistance Genes

In addition to their success as independently functional antibiotics, PPMOs also show potential as combinatorial therapies for standard antibiotics. By targeting resistance genes, PPMO treatment can sensitize resistant strains to their formerly impotent antibiotic treatments. PPMOs targeted to blaT-ampicillin and cml-chloramphenicol resistance genes reduced the MIC of ampicillin and chloramphenicol by 32 and 64 fold, respectively (Figure 9). The quantity of classical antibiotic needed for growth inhibition was reduced when coupled with PPMO treatment. *E. coli* SMS-3-5 growth was inhibited by 32 ug/mL ampicillin when given 32 uM blaT-PPMO co-treatment, and inhibited by 8 ug/mL chloramphenicol when given 32 uM cmlA-PPMO co-treatment. BlaT is a beta-lactamase that hydrolyzes penicillins, ampicillin, and cephalosporins. CmlA is a part of the multidrug efflux pump CMr/MdfA (Bohn and Bouloc, 1998). A PPMO targeted to the tetracycline efflux pump gene *tetA* was much less effective in reducing the MIC of tetracycline by only 2-fold (Figure 10). For *tetA* mediated resistance, the quantity of classical antibiotic needed for growth inhibition

was only slightly reduced when coupled with PPMO treatment. *E. coli* SMS-3-5 growth was inhibited by 32 ug/mL tetracyline when given 8 uM or more of tetA-PPMO co-treatment. This relatively mild effect on antibiotic resistance can be

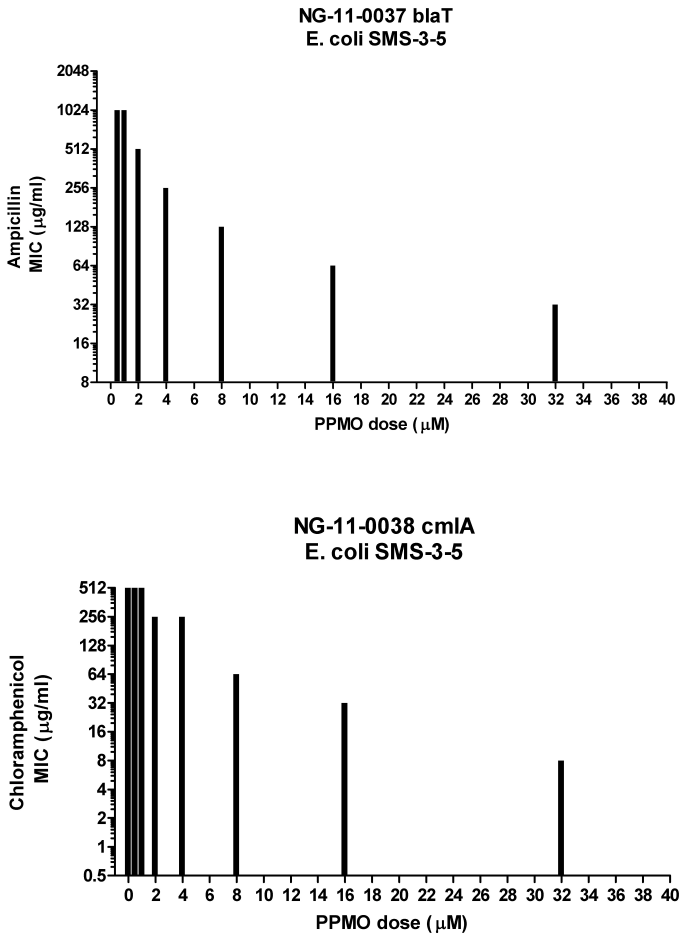

Figure 9. PPMOs Targeted to Resistance Genes Increase Sensitivity to Standard Antibiotics. The environmental *E. coli* strain SMS-3-5 was treated with varying concentrations of two combination therapies: blaT-PPMO with ampicillin, or cmlA-PPMO with chloramphenicol.

attributed to two possibilities discussed previously: firstly, that the target sequence was somehow ineffective in binding the PPMO or interfering with the ribosome, or secondly that some redundant gene compensated for the target's silencing and thereby negated any PPMO effect.

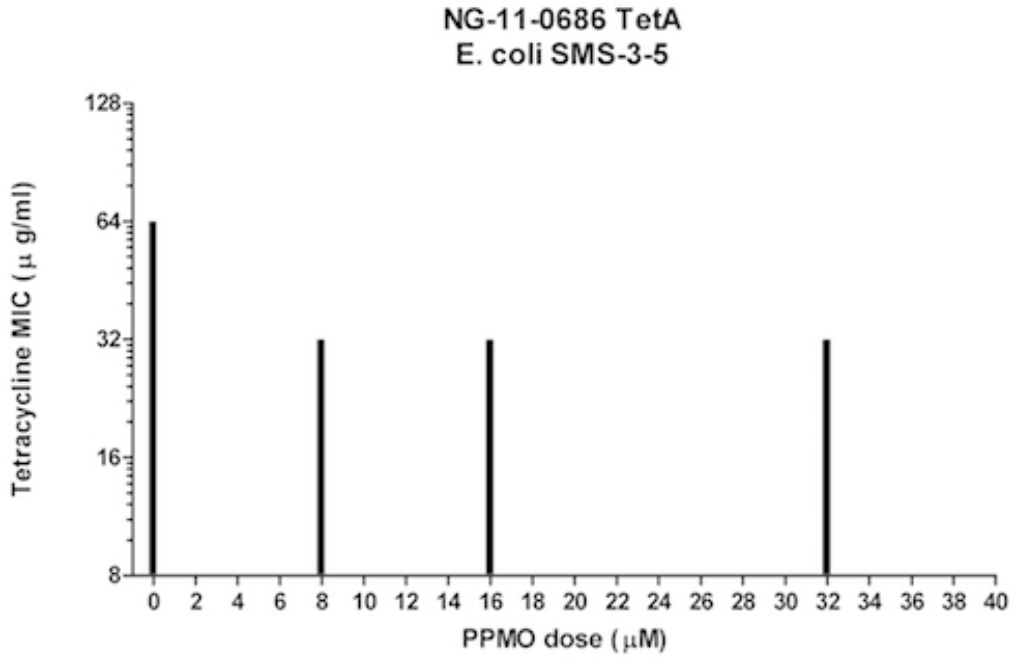

Figure 10. PPMO Targeted to Tetracycline Resistance Gene Increases Tetracycline Sensitivity. The environmental *E. coli* strain SMS-3-5 was treated with varying concentrations tetA-PPMO and tetracycline. The quantity of classical antibiotic needed for growth inhibition was slightly reduced when coupled with PPMO treatment. *E. coli* SMS-3-5 growth was inhibited by 32 ug/mL tetracyline when given 8 uM or more of tetA-PPMO co-treatment. Turbidity values were averaged from triplicate measurement wells as described in Materials and Methods. Results from a single experiment are presented above.

Significant decreases in ampicillin and chloramphenicol resistance in PPMO-treated *E. coli* SMS-3-5 suggested that other *E. coli* strains could show similar sensitivities if treated with similar combinations. To test this hypothesis, our work primarily focused on clinical isolates expressing *NDM-1*, the gene encoding New Delhi metallo-beta-lactamase-1 (NDM-1). NDM-1 is a carbapenemase that confers resistance to a broad range of beta-lactam antibiotics, including the carbapenem drugs of last resort standardly used for antibiotic-resistant bacterial infections. Multiple PPMOs were targeted to NDM-1 sequence regions and combined with various dosages of the carbapenem imipenem to inhibit growth of *NDM-1* positive *E. coli* strains (Figure 11 A-K & data not shown). We measured the MICs of NDM1-PPMOs

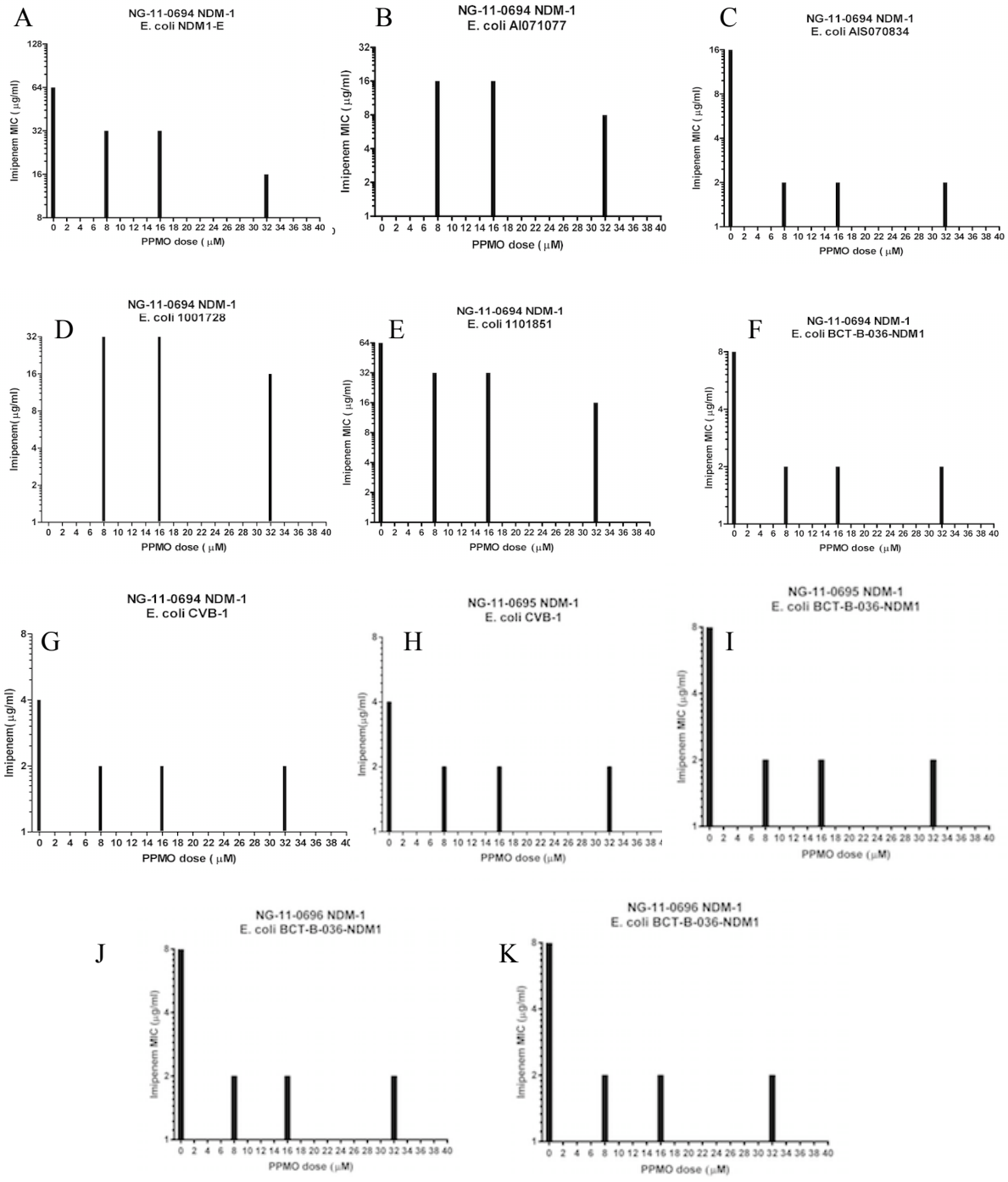

Figure 11. NDM1-PPMOs in *E.* coli BCT-B-036-NDM1 Increase Imipenem Sensitivity. A panel of NDM-1- containing *E. coli* strains were treated with varying concentrations of imipenem and NDM1-PPMOs designed to pair with different hybridization sites on the *NDM-1* mRNA. The figures here show a representative

targeted to various hybridization sequences on the target mRNA in order to determine the optimal positioning of NDM1-PPMOs for gene silencing. The varying susceptibility of the different NDM-1 containing strains to the same NDM1-PPMO was also elucidated using this comparative approach. NDM-1 positive *E. coli* strains experienced reductions of imipenem resistance ranging from two to eight fold, but only at relevantly high concentrations of 11-0694 NDM1-PPMO (Figure 11A-G). The *E. coli* strains dosed with 11-0695 NDM1-PPMO showed a smaller range of imipenem resistance reductions, all of which were between two and four fold (Figure 11H-I and data not shown). The pattern of two to four fold resistance decrease to imipenem was continued in *E. coli* strains treated with 11-0696 NDM1-PPMO (11J-K, data not shown). The greatest reduction in antibiotic resistance was observed for *E. coli* AIS070834 treated with NDM1-PPMO NG-11-0694, *E. coli* AIS070834 treated with NDM1-PPMO NG-11-0695, and *E. coli* CVB-1 treated with NDM1-PPMO NG-11-0696. These combination treatments reduced the strains' imipenem MICs by eight fold. Our data indicated shifts in NDM1 potency to correlate more strongly with strain identity than PPMO positioning, a result demonstrated most clearly by the testing performed in *E. coli* BCT-036-NDM1 (11F, 11I, 11K). All three NDM1-PPMOs decreased imipenem resistance by two fold in this strain despite their slightly different positions relative to the initiation codon of the NDM-1 mRNA. By contrast, the collection of strains treated within each NDM1-PPMO group exhibited varying changes in resistance (11A-K & data not shown).

The low fold-changes of the three previously tested PPMOs motivated development of the new NDM1-PPMO NG-12-0105. NG-12-0105 moved the

position of the PPMO 2-bases upstream of NG-11-0695 to bases -10 through +1 (where the first base of the start codon is +1 and negative numbers indicate the upstream, untranslated region). This PPMO was then tested in combination with the NDM-1 positive *E. coli* AIS070834 due to the relatively large fold changes in carbapenem sensitivity observed from previous experiments (data not shown). Meropenem was used in this experiment because preliminary data had demonstrated this carbapenem to exhibit greater stability in storage than imipenem (data not shown)

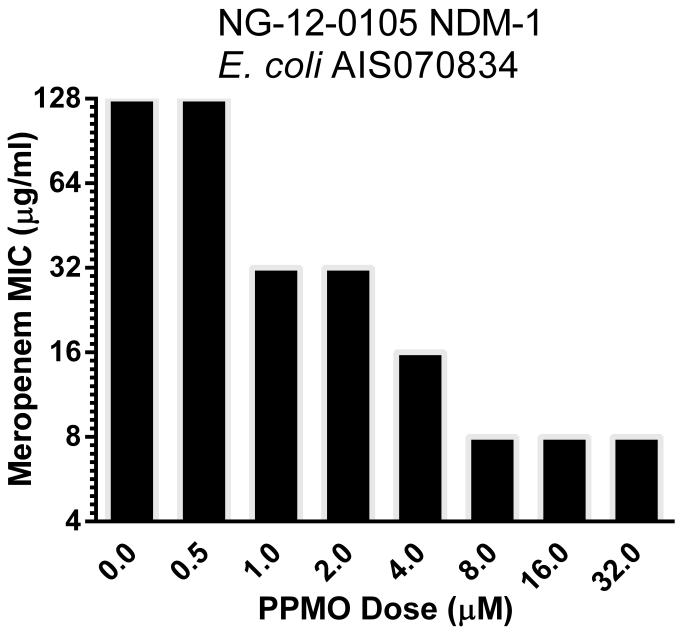

Figure 12. PPMO Targeted to NDM-1 Reduces Meropenem Resistance The clinical *E. coli* isolate AIS070834 was treated with varying concentrations of NDM-PPMO and meropenem.

The quantity of meropenem needed for growth inhibition was reduced by 16 fold when coupled with PPMO treatment. *E. coli* AIS070834 growth was inhibited by 8 ug/mL meropenem when given 8 uM or more of 12-0105 NDM1-PPMO co-treatment. The markedly increased sensitivity restoration can be attributed exclusively to repositioning in this experiment, since previous NDM1-PPMOs in *E. coli*

AIS070834 reduced resistance by a maximum of eight-fold. The three base shift in the 12-0105 NDM1-PPMO was able to reduce the concentrations of antibiotic and PPMO to the clinically relevant doses of 8 uM.

Effect of NDM1-PPMO on NDM-1 mRNA Levels

The effect of PPMO treatment on target mRNA levels was evaluated. NDM1-PPMO was selected because it targets a non-essential gene. NDM1-PPMO was added to growing cultures of *E. coli* AIS070834, which expresses the *NDM-1* gene. Control cultures included no treatment, or an identical concentration of a scrambled sequence PPMO. Samples of the cultures were removed at various times after adding the PPMO, and NDM-1 mRNA was measured by qPCR (Figure 13). Neither NDM1-

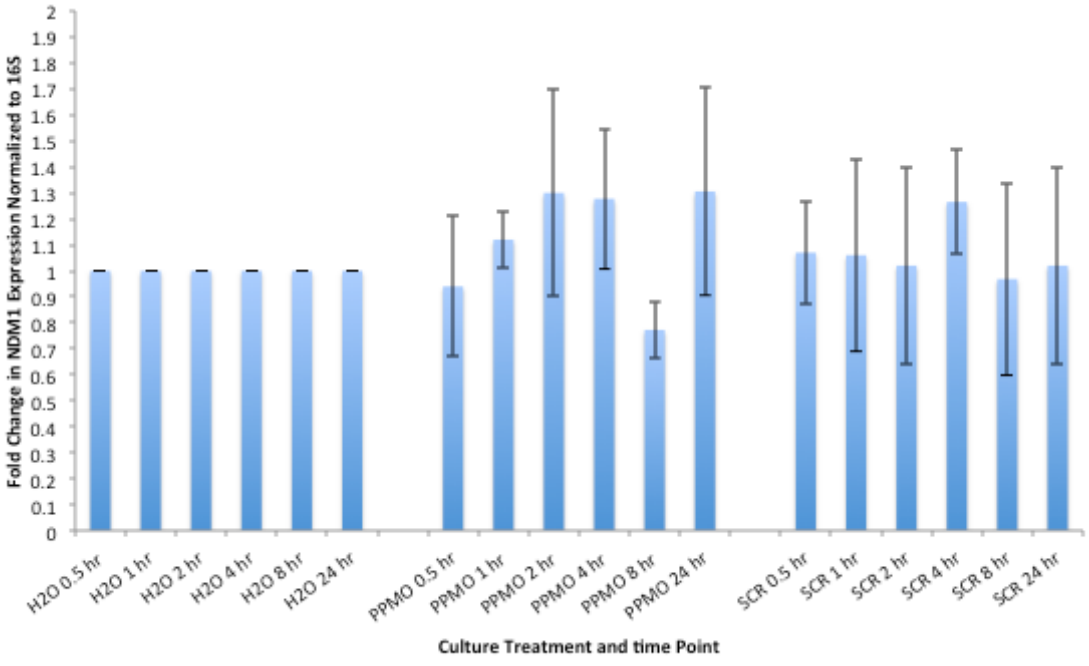

Figure 13. NDM1-PPMO Treatment Does Not Significantly Alter mRNA Levels of the *NDM-1* Gene. *NDM1* containing *E. coli* strain AIS070834 was treated in triplicate with 16 uM NDM-1 targeted PPMO NG-12-0105, 16 uM non-targeted scramble PPMO NG-06-0949, or an equivalent volume of the water vehicle as a control. Statistical analysis of difference between paired treatment groups was performed using a paired student's t-test. No two treatments were significantly different from each other ($p<0.05$).

PPMO nor scrambled PPMO significantly altered the level of of NDM1 mRNA, as confirmed by analysis of the data with a paired student's t-test. Combination therapy data showed inhibition of *NDM1* activity at treatment concentrations as low as 8 uM, indicating the NDM1-PPMO to be effective at the high treatment concentration of 16 uM. The successful silencing of *NDM1* without a correlated decrease in mRNA synthesis indicates that PPMOs function without changing the targeted mRNA level. The stability of mRNA level suggests PPMOs' mode of action does not affect mRNA turnover of the target gene or rate of target mRNA transcription.

Human Tissue Culture Cytotoxicity Assays

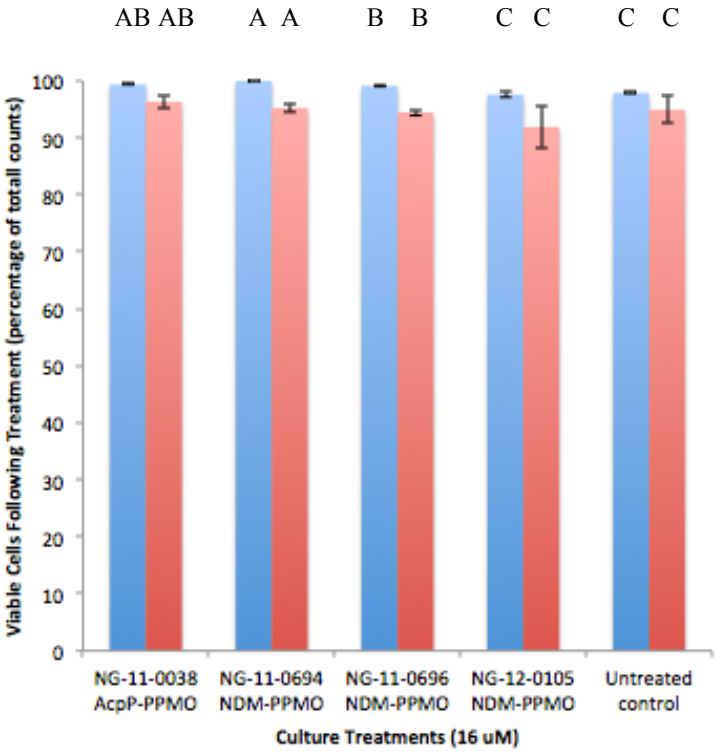

Figure 14. PPMO Treatment Does Not Significantly Affect Human Cell Survival. Human cancer cell lines THP-1 (blue columns) and A549 (red columns) were cultured with or without 10 uM PPMO treatments for 48 hours.. Statistical analysis of difference between treatment groups was performed using a student's paired t-tests. Treatments not connected by the same letter are significantly different ($p<0.05$). Results from a single experiment are presented above.

The safety of PPMOs was assessed by measuring the toxicity in human tissue cultures. THP-1 is derived from human monocytes and A549 from human lung cells PPMOs were added at 10 μM to tissue cultures, and the viability was measured after 48 hours of exposure. Controls cultures were treated with scrambled PPMO, free $(RXR)_4XB$ peptide, non-conjugated PMO, or untreated. The results show that none of the PPMOs tested reduced viability of either cell line, and student's paired t-test analysis (Figure 14). Scrambled PPMO, free peptide and non-conjugated PMO had no effect on viability (data not shown). This suggests that PPMOs are not toxic, at least as measured in tissue culture. Further tests in animals will be required to establish a more comprehensive toxicity profile.

CHAPTER 5 - DISCUSSION

The extensive use of antibiotics worldwide has selected for a population of pathogens increasingly resistant to standard antimicrobial therapies. Growing numbers of bacterial pathogens are exhibiting multi-drug resistance, and the emergence of extremely-resistant strains lacking sensitivity to all known compounds has become a significant medical problem (Boucher et al., 2013; Tenover, 2001, Smith and Coast, 2013). The prevalence of microbial resistance to current therapies necessitates the investigation and development of novel antibiotic compounds to which bacteria are still broadly sensitive. PPMOs can be bactericidal by silencing critical microbial genes or restoring standard antibiotic sensitivity through silencing resistance genes. My thesis has identified PPMOs targeted to essential genes that can inhibit *E. coli* growth and to antibiotic resistance genes that can restore susceptibility to standard antibiotics.

Essential Gene Screening for PPMO Drug Targets in Rich and Minimal Media

Use of PPMOs designed to bind the essential genes *acpP* and *murA* demonstrated the strongest inhibition in the greatest number of strains. Most importantly, PPMOs targeted to these genes were able to suppress growth of resistant *E. coli* strains at concentrations comparable to standard antibiotics. The potency of AcpP-PPMOs and the MurA-PPMO at clinical dose levels suggest *acpP* and *murA* to be promising targets for future development of PPMO antibiotics. The efficacy of AcpP-PPMOs can be attributed to *acpP*'s crucial role as a carrier of acyl intermediates during fatty acid and polyketide biosynthesis (Byers and Gong, 2007). MurA is known to control an essential early step in the synthesis of the peptidoglycan

wall, rendering it a crucial gene for bacterial survival (Gautam et al., 2011). Both targets also possess a high degree of sequence conservation across Gram-positive and Gram-negative bacteria, rendering AcpP-PPMOs and MurA-PPMO broadly applicable antimicrobials (Bensen et al., 2012; Byers and Gong, 2007). This broad potency has been demonstrated by AcpP-PPMO growth suppression of numerous bacteria, including *S. enterica*, *B. cepacia,* and *A. baumannii* (Tilley et al., 2006, Greenberg et al., 2010, Geller et al., 2013). Although MurA-PPMOs have not yet been tested *in vivo*, there exists a standard antibiotic fosfomycin which is known to target the *murA* gene product. Fosfomycin is a natural product made by some *Streptomyces* species. Its mechanism of action is an alkylation of a cysteine residue in the active site of MurA. This inactivation of MurA is fatal for diverse pathogens including *Haemophilus influenza, Mycobacterium tuberculosis,* and *Chlamydia trachomatis* (Bensen et al., 2012). Our data suggests *E. coli* strains are similarly susceptible to prevention of cell wall synthesis through silencing of *murA*.

Despite the success of *acpP* and *murA* targeting, PPMOs against numerous other major biological pathway genes failed to inhibit *E. coli* replication. The failure of these PPMOs could be attributed to ineffective binding near a secondary mRNA structure or compensatory activity by redundant genes not suppressed by the oligomer. However, the sheer quantity of unsuccessful targets suggests physiological factors may be contributing to the inconsistency of PPMO inhibition between targets. PPMO efficacy may be influenced by differences in mRNA turnover and abundance for a particular target gene. *E. coli* mRNAs are known to be rapidly decay through digestion by bacterial ribonucleases. Thus if a particular target mRNA is

constitutively degraded and resynthesized at a high rate then the brief arrest of translation induced by PPMO binding may not make a large difference in total gene expression. Similarly, if a specific target mRNA is kept at high abundance in the bacterial cell then clinically relevant doses of PPMO treatment may not be sufficient to suppress enough target transcripts for change gene expression levels overall. By contrast, target genes with constitutively low mRNA turnover rates and abundance may be more vulnerable to the inhibitory effects of PPMO treatment since the bacteria is less prepared to compensate for transcript degradation. Thus the extent to which each gene must be silenced in order to inhibit growth may be different for each gene Another possibility may be that the correct positioning of the PPMO to the target mRNA is slightly different for each gene or differs for the same gene between species. However, the closely related nature of the strain panel used in our experiments makes nucleotide sequence differences between genes encoding the same product to be less expected.. For these reasons the inter-strain differences in PPMO efficacy, as exemplified clearly in *E. coli* SMS-3-5's unique susceptibility to GapA-PPMO, are likely due to differences of target mRNA abundance and turnover between *E. coli* strains (Figure 7).

The contextual characteristics of gene essentiality could be another source of variation in PPMO efficacy. The essentiality of gene has been observed to change depending on such fluid parameters as nutrient levels, carbon sources, and environmental stresses (Umland et al., 2012; D'Elia et al., 2009). For example, the exogenous metabolites in rich media enable quick rescue of mutations since the cell does not have to manufacture components of biosynthetic pathways themselves

(D'Elia et al., 2009). The nonessentiality of these manufacturing genes in rich media thus alter the set of genes actually necessary for bacterial growth. Initial screening in our work was performed in Mueller Hinton II broth, a nutrient dense media not at all like the sparse host environment. The rich media likely compensated for the loss of putative essential gene expression. Subsequent target screenings were performed in MOPS Minimal Media, a culture broth using only trace nutrient elements to sustain bacterial growth. Our data showed that PPMOs successful in rich media were even more potent in a minimal nutrient environment. More importantly, the Adk-PPMO and InfA-PPMO were able to inhibit *E. coli* growth at a clinically relevant concentration in the MOPS broth. The potency of Adk-PPMO, in minimal but not rich media, could be partially attributed to its role as a regulator of bacterial responses to stress and food stimuli. The low-stress, consistently favorable nutrient state of Mueller Hinton II media likely necessitated much less regulation than the varied living conditions of bacteria outside the laboratory. The increased efficacy of InfA-PPMO is less understood, since *infA* is a general translation initiation factor without a known, specific function. Nonetheless, as delineated by D'Elia et al. in her 2009 study, fewer translational events may need to occur in a rich media environment since metabolites do not need to be synthesized *de novo*. However, both genes have previously been identified as essential in rich media (Baba et al., 2006). Therefore the absence of growth inhibition following PPMO treatment in Mueller-Hinton II broth is more likely an indicator of target mRNA levels. Target genes with low mRNA abundance or turnover may become more critical in minimal media environments where high gene expression is necessary for bacterial survival. The partial inhibition

of a gene target mediated by clinical doses of PPMO may not make a significant difference in the low stress environment of rich media, but may cripple important cellular machinery in minimal media by just a small decrease in target translation. Regardless, the overall increased efficacy of PPMOs in minimal media suggests that laboratory conditions more similar to the *in vivo* host environment could identify effective gene targets obscured by rich media conditions. Clearly what is needed next is an *in vivo* study to see if PPMOs that were potent only in minimal medium are effective in the host environment. In addition to approximating the low nutrient state of hosts, future screenings could also employ immune factors and temperature fluctuations to identify other stress response gene targets for PPMO therapy.

Resistance Gene Screening for PPMO Drug Targets in Combination with Standard Antibiotics

Essential gene suppression enables PPMOs to act as independent antimicrobials, but PPMOs targeted to resistance genes can be co-administered with standard antibiotics to create effective combination therapies. PPMO-mediated silencing of resistance genes restores sensitivity to a class or particular type of antibiotic, enabling treatment with that antibiotic to inhibit bacterial growth at clinically relevant concentrations again. My results showed that PPMOs specifically targeted to genes that encode resistance to ampicillin or chloramphenicol reduced the MIC of these antibiotics in various strains of *E. coli*. This supports the hypothesis that PPMOs may be used as adjuncts with standard antibiotics to combat antibiotic-resistant bacteria. However, it should be noted that the concentration of PPMO required to reduce the MIC of standard antibiotic was frequently higher than what is thought to be achievable in serum. Nevertheless, topical applications of PPMO, such

as an aerosol delivery to the lungs of pneumonia patients may achieve significantly higher local concentrations of PPMO, perhaps in the range needed for efficacy *in vitro*. In addition, resistant nosocomial *E. coli* strains are usually unique emergences not yet characterized. To obtain data more relevant to treatment of pathogenic *E. coli* strains, combination therapies of PPMO and classical antibiotics were applied to the resistant clinical isolate *E. coli* AIS070834.

E. coli AIS070834 is a multidrug-resistant strain from the collection of NDM-1 positive isolates kept at the Centers for Disease Prevention and Control. The strain's remarkable resistance to most antibiotic treatments is attributed to its possession of the New Delhi metallo-beta-lactamase-1 (NDM-1) gene. NDM-1 is a recently discovered zinc metallo-beta-lactamase capable of hydrolyzing all penicillins, cephalosporins, and carbapenems (Walsh et al., 2005). Although NDM-1 can be taken up as an independent gene, bacteria frequently acquire NDM-1 through transformation with plasmids. These plasmids usually co-harbor multiple, variable resistance determinants such as methylases, synthases, ribosyltransferases, and acetyltransferases that confer insensitivity to most antibiotic classes. A few NDM-1 bearing plasmids also encode other types of beta-lactamases and carbapenemases. The resistance mechanisms encoded by NDM-1 and the plasmids that carry it allow NDM-1 positive bacteria to usually resist treatment with all beta-lactam based antibiotics, quinolones, chloramphenicol, rifampicin, aminoglycosides, sulfonamides, and macrolides (Normann et al., 2011; Poirel et al., 2011). In addition to the variety of resistances conferred with NDM-1, its frequent incorporation into promiscuous plasmids enable the gene to integrate into a broad spectrum of host species including

Klebsiella, Proteus, Enterobacter, Citrobacter, Acinetobacter, Pseudomonas, Stenotrophomonas, Aeromonas, Shigella, and *Vibrio cholera*. Epidemiological studies have found NDM-1 isolates all over the world since 2010, indicating this gene to be rapidly spreading across the continents (Nordmann et al., 2011). The comprehensive antibiotic immunity and ease of acquisition has made NDM-1 a resistance gene of critical concern since its discovery in 2009. Subsequently, targeting this gene for PPMO-antibiotic combination treatment could yield a novel antimicrobial therapy capable of broad potency for all strains possessing NDM-1. The model system tested in this paper showed that the synergistic effects of PPMO and meropenem in combination lowered the effective dose for both compounds significantly. By treating in combination, clinically relevant concentrations of NDM1-PPMO and meropenem inhibited the growth of NDM-1 positive *E. coli* AIS070834. The success of this combination treatment suggests that these kinds of co-treatments might be able to return infectious disease therapy to the age of antibiotics, since sensitivity to well-established classical compounds could be restored with PPMOs. NDM-1 is just one of many multiple-resistance gene targets that could be silenced through the employment of PPMO combination therapies. Efflux pump genes constitute another potential target for broadly useful, pathogen-specific PPMO inhibition that could restore bacterial sensitivity to classical antibiotics.

Elucidation of PPMO Mechanism of Action in Bacteria

In addition to providing proof of concept for combination therapies in a key clinical context, the NDM1-PPMO also facilitated examination of real time PPMO effects without the cell lethality characterizing essential-gene-targeted oligomers. The

NDM1-PPMO's ability to sensitize *E. coli* AIS070834 to meropenem demonstrated the oligomer to be functional at a particular concentration in a particular pathogenic environment. Replicating this environment without the addition of meropenem enabled investigation of the molecular actions of a successful PPMO. Current literature still presents some confusion over PPMOs' precise mechanism of gene inhibition through translational arrest., . A 2008 paper by Patel et. al studying PPMO inhibition of porcine reproductive and respiratory syndrome virus found treatment with effective oligomer to significantly lower target RNA levels (Patel et al., 2008). However, Neuman et al.'s study of PPMO function in Arenaviridae suggested that PPMO inhibition of viral RNA synthesis was not sufficient to stop virus replication. Instead, only PPMOs interfering with translation were effective against the viruses (Neuman et al., 2011). Orthogonally, eukaryotic gene targeted PPMOs are employed for the very reason that they do not trigger RNA degradation in that cellular context. PPMOs are used in eukaryotes to inhibit or redirect pre-mRNA splicing by blocking splice sites (Moulton et al., 2008; Douglas and Wood, 2013). Reporter gene assays performed with luciferase and beta-galactosidase have quantitatively confirmed the decrease in translation indirectly proven by loss of PPMO target function (Tilley et al., 2006; Geller et al., 2003). However, transcriptional studies of mRNA levels following treatment with effective or ineffective PPMOs have not yet been published.

To clarify the mechanism of action of PPMOs, this study used real-time quantitative PCR to measure changes of NDM-1 mRNA levels in cells treated with NG-12-0105 NDM1-PPMO. Analysis of mean mRNA levels using a student's t-test showed there to be no significant difference in NDM-1 mRNA between *E. coli*

AIS070834 cultures treated with NDM1-PPMO, scrambled nonsense PPMO, or the water vehicle. These data suggest PPMOs affect neither the transcription or mRNA degradation of their target genes. These data support the current model of PPMO action, which postulates their binding to block mRNA and sterically hinder ribosomal activity to inhibit gene expression. Previous antisense therapies – such as RNAi, siRNA, and antisense gapmer oligonucleotide based drugs – acted through degradation of mRNA by recruiting the multiprotein RNA-induced silencing complex RISC (Kole et al., 2012; Kurreck et al., 2003). The most widely studied modified oligonucleotides, phosphorothioates, also act through mRNA degradation by recruiting RNase H to their target mRNA (Chan et al., 2006; Mansoor et al., 2008). By contrast, phosphorodiamidate morpholino oligomers were never designed to form cleavable complexes with RNA (Summerton and Weller, 1997). The data collected in this study suggests that PPMOs inhibit gene expression not by interfering with transcription nor altering the abundance or turnover rate of target mRNA. This suggests that the mechanism of action of PPMOs is inhibition of translation. The next experimental step should be demonstration by mass spectrometry, two dimensional gel electrophoresis, or Western blot that the level of NDM-1 protein is decreased in cultures treated with the NDM1-PPMO. An antibody to NDM-1 has recently become commercially available, rendering convenient protein immunoblotting of our target gene now possible.

Toxicity of PPMOs in Human Tissue Culture

The safety of PPMOs must be evaluated before they can proceed to human clinical trials. As a preliminary step, we have tested some of the antibacterial PPMOs

for toxicity in tissue culture using two very different cell types. Our results showed that all of the PPMOs tested did not significantly reduce viability of either cell type. We are aware that testing for toxicity in tissue culture is not a substitute for animal testing, and cannot replicate the complex environment inherent in an animal. However, the stability of cancer cell modeling provides a preliminary foundation for future toxicity studies. An additional assessment of toxicity through hemolysin tests of our PPMOs would be another method of strengthening our tentative conclusions about oligomer nontoxicity.

Although the toxicity of antibacterial PPMOs have never been tested in animals, there exist some studies conducted on similar PPMOs. Adams et al. monitored the toxicity of a PPMO 20-bases in length conjugated to the $(RXR)_4XB$ peptide used in most of our antibacterial PPMOs. They found no apparent signs of toxicity in rats treated with the clinically relevant 15 mg/kg PPMO dosage, although the toxic indicators lethargy, weight loss, and elevated blood urea nitrogen counts all manifested at the 150 mg/kg PPMO dosage (Adams et al., 2007). Similarly, Stein et al. observed little impact on overall health from 10 mg/kg PPMO treatments of mice (Stein et al., 2008). These studies established a baseline toxicity for PPMOs. Despite the aggregation of PPMO seen in mouse spleens and livers, no significant damage to the organs was observed in histopathology experiments. In addition, mice continued to exhibit healthy, standard behaviors throughout and following these PPMO treatments. The human cancer cell line employed in this thesis showed similarly negligible toxicity effects even after 48 hours of high concentration PPMO treatment. Analysis of the mean viable cell percentage from plates treated with 16 uM PPMO or

water vehicle revealed there to be no significant difference in cell survival following PPMO exposure. The lack of toxicity even at concentrations 2-4 times the therapeutic dose suggests that PPMOs possess a safety profile acceptable for more advanced clinical testing.

CHAPTER 6 - CONCLUSIONS

PPMOs constitute an exciting set of new molecular tools for therapeutic development. Their specificity, stability, relative ease of synthesis, and highly customizable design render them potent antibiotics capable of acting through numerous gene targets across various bacterial species. The data collected in this study suggest several avenues for further PPMO investigation, including the specific genes *acpP*, *murA*, and *NDM-1*. Through multiple experimental techniques, this thesis demonstrates the potency and safety of these future therapeutics. However, the relative novelty of the PPMOs necessarily requires extensive further research before bringing any compounds to market. Future studies must assess in more comprehensive toxicology models the potential side effects of exposure to PPMOs, determine the optimum delivery routes for PPMO therapy administration, and explore potential mechanisms of PPMO resistance in target bacteria. Additionally, the limited nature of the single-gene-silencing approach suggests future research might be directed toward developing a broader spectrum PPMO. Much work remains to be done for the refinement of antibacterial PPMOs, but present data suggest these compounds may be a powerful and adaptable approach for a new age of antibiotic treatments.

BIBLIOGRAPHY

Amantana, A., Moulton, H., Cate, M., Reddy, M., Whitehead, T., Hassinger, J., Youngblood, D., and Iversen, P. (2007). Pharmacokinetics, biodistribution, stability, and toxicity of a cell-penetrating peptide-morpholino oligomer conjugate. Bioconj Chem *18*, 1325-1331.

Baba, T., Ara, T., Hasegawa, M., Takai, Y., Okumura, Y., Baba, M., Datsenko, K., Tomita, M., Wanner, B., and Mori, H. (2006). Construction of *Escherichia coli* K-12 in-frame single-gene knockout mutants: the Keio collection. Mol Sys Bio *doi:* 10.1038/msb4100050

Bensen, D., Rodriguez, S., Nix, J., Cunningham, M., and Tari, L. (2012). Structure of MurA (UDP-N-acetylglucoasamine enolpyruvyl transferase) from *Vibrio Fischeri* in complex with substrate UDP-N-acetylglucosamine and the drug fosfomycin. Struct Bio and Crystal Comm *68*, 382-385.

Bohn, C., and Bouloc, P. (1998). The *Escherichia coli cmlA* gene encodes the multidrug efflux pump Cmr/MdfA and is responsible for isopropyl-beta-D-thiogalactopyranoside exclusion and spectinomycin sensitivity. J Bacteriol *180*, 6072-6075.

Boucher, H.W., Talbot, G.H., Benjamin, D.K., Bradley, J., Guidos, R.J., Jones, R.N., Murray, B.E., Bonomo, R.A., Gilbert, D., and Infectious Diseases Society of America. (2013). 10 x '20 Progress--Development of New Drugs Active Against Gram-Negative Bacilli: An Update From the Infectious Diseases Society of America. Clin Infect Dis *56*, 1685-1694.

Byers, D., and Gong, H. (2007). Acyl carrier protein: Structure-function relationships in a conserved multifunctional protein family. Biochem and Cell Bio *85*, 649-662.

Campbell, M.A., and Wengel, J. (2011). Locked vs. unlocked nucleic acids (LNA vs. UNA): contrasting structures work towards common therapeutic goals. Chem Soc Rev *40*, 5680-5689.

Chan, J., Lim, S., and Wong, W. (2006). Antisense oligonucleotides: From design to therapeutic application. Clin and Exp Pharma and Physio *33*, 533-540.

Clinical and Laboratory Standards Institute. (2006). Methods for dilution antimicrobial susceptibility tests for bacteria that grow aerobically - Seventh edition: Approved standard M7-A7. CLSI, Wayne, PA, USA.

Costelloe, C., Metcalfe, C., Lovering, A., Mant, D., and Hay, A.D. (2010). Effect of antibiotic prescribing in primary care on antimicrobial resistance in individual patients: systematic review and meta-analysis. BMJ *340*, c2096.

de Bernardinis, V., Vallenet, D., Castelli, V., Besnard, M., Pinet, A., Cruaud, C., samair, S., Lechaplais, C., Gyapay, G., richez, C., Durot, M., Kreimeyer, A., Le Fevre, F., Schachter, V., Pezo, V., Doring, V., Scarpelli, C., Medigue, C., Cohen, G., Marliere, P., Salanoubat, M., and Weissenbacj, J. (2008). A complete collection of single-gene deletion mutants of *Acinetobacter baylyi* ADP1. Mol Syst Bio doi: 10.1038/msb.2008.10.

Deere, J., Iversen, P., and Geller, B. (2004). Phosphorodiamidate morpholino oligomer length and target position effects on gene-specific inhibition in *Escherichia coli*. Antimicro Agents & Chemo *49*, 249-255.

Douglas, A., and Wood, M. (2013). Splicing therapy for neuromuscular disease. Mol Cell Neurosci *56*, 169-185.

Fischbach, M.A., and Walsh, C.T. (2009). Antibiotics for emerging pathogens. Science *325*, 1089-1093.

Gautam, A., Rishi, P., and Tweari, R. (2011). UDP-N-acetylglucosamine enolpyruvyl transferase as a potential target for antibacterial chemotherapy: recent developments. Appl Microbio Bio tech *92*, 211-225.

Geller, B., Deere, J., Stein, D., Kroeker, A., Moulton, H., and Iversen, P. (2003). Inhibition of gene expression in *Escherichia coli* by antisense phosphorodiamidate morpholino oligomers. Antimicro Agents & Chemo *47,* 3233-3239.

Geller, B.L. (2005). Antibacterial antisense. Curr Opin Mol Ther *7*, 109-113.

Geller, B., Deere, J., Stein, D., Kroeker, A., Moulton, H., and Iversen, P. (2003). Inhibition of gene expression in *Escherichia coli* by antisense phosphorodiamidate morpholino oligomers. Antimicro Agents & Chemo *47*, 3233-3239.

Geller, B., Marshall-Batty, K., Schnell, F., McKnight, M., Iversen, P., and Greenberg, D. (2013). Gene-silencing antisense oligomers inhibit *Acinetobacter* growth in vitro and in vivo. J Infect Diseases *208*: 1553-1560.

Giedraitiene, A., Vitkauskiene, A., Naginiene, R., and Pavilonis, A. (2011). Antibiotic resistance mechanisms of clinically important bacteria. Medicina (Kaunas) *47*, 137-146.

Good, L., Awasthi, S., Dryselius, R., Larsson, O., and Nielsen, P. (2001). Bactericidal antisense effects of peptide-PNA conjugates. Nature Biotech *19*, 360-364.

Greenberg, D., Marshall-Batty, K., Brinster, L., Zarember, K., Shaw, P., Mellbye, B., Iversen, P., Holland, S., and Geller, B. (2010). Antisense phosphorodiamidate morpholino oligomers targeted to an essential gene inhibit *Burkholderia cepacia* complex. J Infect Diseases *201*, 1822-1830.

Hatamoto, M., Ohashi, A., Imachi, H. (2010). Peptide nucleic acids (PNAs) antisense effect to bacterial growth and their application potentiality in biotechnology. Appl Microbio Bio tech *87*, 397-402

Heasman, J. (2002). Morpholino oligos: Making sense of antisense. Dev Bio *243*, 209-214.

Henriques, S., Melo, M., and Castanho, M. (2006). Cell-penetrating peptides and antimicrobial peptides: how different are they? Biochem J *399*, 1-7.

Jepsen, J., Sorensen, M., and Wengel, J. (2004). Locked nucleic acid: a potent nucleic acid analog in therapeutics and biotechnology. Oligonucleotides *14*, 130-146.

Kole, R., Krainer, A.R., and Altman, S. (2012). RNA therapeutics: beyond RNA interference and antisense oligonucleotides. Nat Rev Drug Discov *11*, 125-140.

Koppelhus, U., and Nielsen, P. (2003). Cellular Delivery of Peptide Nucleic Acid (PNA).

Malerba, A., Boldrin, L., and Dickson, G. (2011). Long-term systemic administration of unconjugated morpholino oligomers for therapeutic expression of dystrophin by exon skippin in skeletal muscle: implications for cardiac muscle integrity. Nuc Acid Ther *21*, 293-298.

Mansoor, M., and Melendez, A.J. (2008). Advances in antisense oligonucleotide development for target identification, validation, and as novel therapeutics. Gene Regul Syst Bio *2*, 275-295.

Martinez, M., Mendoza, D., and Schujman, G. (2010). Transcriptional and functional characteristics of the gene encoding acyl carrier protein in *Bacillus subtilis*. Micro *156*, 484-495.

Mellbye, B., Puckett, S., Tilley, L., Iversen, P., and Geller, B. (2009). Variations in amino acid composition of antisense peptide-phosphorodiamidate morpholino oligomer affect potency against *Escherichia coli* in vitro and in vivo. Antimicro Agents & Chemo *53*, 525-530.

Moulton, H., and Moulton, J. (2010). Morpholinos and their peptide conjugates: Therapeutic promise and challenge for Duchenne muscular dystrophy. Biochim et Biophys Acta *1798*, 2296-2303.

Moulton, H., Nelson, M., Hatlevig, S., Reddy, M., and Iversen, P. (2004). Cellular uptake of antisense morpholino oligomers conjugated to arginine-rich peptides. Bioconjugate Chem *15*, 290-299.

Moulton, J., and Yan, Y. (2008). Using morpholinos to control gene expression. Curr Pro in Mol Bio *26.8.1-26.8.29*.

Neuman, B., Stein, D., Kroeker, A., Churchill, M., Kim, A., Kuhn, P., Dawons, P., Moulton, H., Bestwick, R., Iversen, P., and Buchmeier, M. (2005). Inhibition, escape, and attenuated growth of severe acute respiratory syndrome coronavirus treated with antisense morpholino oligomers. J Virology *79*, 9667-9676.

Neuman, B., Bederka, L., Stein, D., Ting, J., Moulton, H., and Buchmeier, M. (2011). Development of peptide-conjugated morpholino oligomers as pan-arenavirus inhibitors. Antimicro Agents Chemo *55*, 4631-4638.

Nordmann, P., Poirel, L., Walsh, T., and Livermore, D. (2011). The emerging NDM carbapenemases. Trends in Micro *19*, 588-595.

Panchal, R., Geller, B., Mellbye, B., Lane, D., Iversen, P., and Bavari, S. (2012). Peptide conjugated phosphorodiamidate morpholino oligomers increase survival of mice challenged with Ames *Bacillus anthracis*. Nuc Acid Ther *22*, 316-322.

Patel, D., Opriessnig, T., Stein, D., Halbur, P., Meng, X., Iversen, P., and Zhang, Y. (2008). Peptide-conjugated morpholino oligomers inhibit porcine reproductive and respiratory syndrome virus replication. Antiviral Research *77*, 95-107.

Peleg, A., Seifert, H., and Paterson, D. (2008). *Acinetobacter baumannii*: Emergence of a successful pathogen. Clin Micro Rev *21*, 538-582.

Petersen, M., Bondensgaard, K., Wengel, J., and Jacobsen, J.P. (2002). Locked nucleic acid (LNA) recognition of RNA: NMR solution structures of LNA:RNA hybrids. J Am Chem Soc *124*, 5974-5982.

Poirel, L., Schrenzel, J., Cherkaoui, A., Bernabeu, S., Renzi, G., and Normand, P. (2011). Molecular analysis of NDM-1-producing enterobacterial isolates from Geneva, Switzerland. J Antimicro Chemo *66*, 1730-1733.

Puckett, S., Reese, K., Mitev, G., Mullen, V., Johnson, R., Pomraning, K., Mellbye, B., Tilley, L., Iversen, P., Freitag, M., and Geller, B. (2012). Bacterial resistance to antisense peptide phosphorodiamidate morpholino oligomers. Antimicro Agents & Chemo *56*, 6147-6153.

Rathee, P., Rathee, D., Hood, A., Kumar, V., and Rathee, S. (2012). Peptide Nucleic Acids:An Overview. The Pharma Innovation *1*, 25-42.

Smith, R., and Coast, J. (2013). The true cost of antimicrobial resistance. BMJ *346*.

Stein, D., Foster, E., Huang, S., Weller, D., and Summerton, J. (1997). A specificity comparison of four antisense types: Morpholino, 2'-O-methyl RNA, DNA, and phosphorothioate DNA. Antisense and Nuc Acid Drug Dev *7*, 151-157.

Stein, D., Huang, C., Silengo, S., Adams, A., Crumley, S., Blouch, R., Iversen, P., and Kinney, R. (2008). Treatment of AG129 mice with antisense morpholino oligomers increases survival time following challenge with dengue 2 virus. J Antimicr Chemo *62*, 555-565.

Summerton, J. (1999). Morpholino antisense oligomers: The case for an RNase H-independent structural type. Biochim Biophys Acta *1489*,141–158.

Summerton, J., and Weller, D. (1997). Morpholino antisense oligomers: Design, preparation, and properties. Antisense & Nuc Acid Drug Dev *7*, 187-195.

Summerton, J., Stein, D., Hunag, S., Matthews, P. Weller, D., and Partridge, M. (1997). Morpholino and phosphorothioate antisense oligomers compared in cell-free and in-cell systems. Antisense and Nuc Acid Drug Dev *7*, 63-70.

Tenover, F.C. (2001). Development and spread of bacterial resistance to antimicrobial agents: An overview. Clin Infect Dis *33*, S108-S115.

Tilley, L., Hine, O., Kellogg, J., Hassinger, J., Weller, D., Iversne, P., and Geller, B. (2006). Gene-specific effects of antisense phosphorodiamidate morpholino oligomer-peptide conjugates on *Escherichia coli* and *Salmonella enterica* serovar typhimurium in pure culture and in tissue culture. Antimicro Agents & Chemo *50*, 2789-2796.

Tillotson, G., and Theriault, N. (2013). New and alternative approaches to tackling antibiotic resistance. F1000Prime *5*, doi:10.12703/P5-51.
Veedu, R.N., and Wengel, J. (2009). Locked nucleic acid as a novel class of therapeutic agents. RNA Biol *6*, 321-323.

Umland, T., Schultz, W., MacDonald, U., Olson, R., and Russo, T. (2012). *In vivo*-validated essential genes identified in *Acinetobacter baumannii* by using human ascites overlap poorly with essential genes detected on laboratory media. mBio ASM *3*, e00113-12.

Vester, B., and Wengel, J. (2004). LNA (locked nucleic acid): high-affinity targeting of complementary RNA and DNA. Biochemistry *43*, 13233-13241.

Wahlestedt, C., Salmi, P., Good, L., Kela, J., Johnsson, T., Hokfelt, T., Broberger, C., Porreca, F., Lai, J., Ren, K., Ossipove, M., Koshkin, A., Jakobsen, N., Skouv, J., Oerum, H., Jacobsen, M., and Wengel, J. (2000). Potent and nontoxic antisense oligonucleotides containing locked nucleic acids. PNAS *97*, 5633-5638.

Walsh, T., Toleman, M., Poirel, L., and Nordmann, P. (2005). Metallo-beta-lactamases: the quiet before the storm? Clin Micro Rev *18*, 306-325.

Wang, G., and Xu, X. (2004). Peptide nucleic acid (PNA) binding-mediated gene regulation. Nature Cell Res *14*, 111-116.

Wu, R., Youngblood, D., Hassinger, J., Lovejoy, C., Nelson, M., Iversen, P., and Moulton, H. (2007). Cell-penetrating peptides as transporters for morpholino oligomers: effects of amino acid composition on intracellular delivery and cytotoxicity. Nuc Acids Research *35*, 5182-5191.

Yeaman, M., and Yount, N. (2003). Mechanisms of antimicrobial peptide action and resistance. Pharmacol rev *55*, 27-55.

Zamecnik, P.C., and Stephenson, M.L. (1978). Inhibition of rous sarcoma virus replication and cell transformation by a specific oligodeoxynucleotide. Proc Natl Acad Sci USA *75*, 280-284.

Zhang, B., Dong, H., Stein, D., and SHi, P. (2008). Co-selection of West Nile virus nucleotides that confer resistance to an antisense oligomer while maintaining long-distance RNA/RNA base-pairings. Virology *382*, 98-106.

Zhou, J., Chen, Y., Tabibi, S., Alba, L., Garber, E., and Saiman, L. (2007). Antimicrobial susceptibility and synergy studies of *Burkholderia cepacia* complex isolated from patients with cystic fibrosis. Antimicro Agents & Chemo *51*, 1985-1088.